Journal of Physical and Chemical Reference Data

Wide-Ranging Reference Correlations for Dilute Gas Transport Properties Based on *Ab Initio* Calculations and Viscosity Ratio Measurements

Xiong Xiao (肖雄), Darren Rowland, Saif Z. S. Al Ghafri, Eric F. May*

Fluid Science & Resources Division, Department of Chemical Engineering, The University of Western Australia, Crawley, WA 6009, Australia

*Corresponding author

Email addresses: xiong.xiao@research.uwa.edu.au (Xiong Xiao), darren.rowland@uwa.edu.au (Darren Rowland), saif.alghafri@uwa.edu.au (Saif Z.S. Al Ghafri), eric.may@uwa.edu.au (Eric F. May)

Abstract

Combined use of experimental viscosity ratios together with *ab initio* calculations for helium have driven significant improvements in the description of dilute gas transport properties. Here we first use improvements made to *ab initio* helium calculations to update viscosity ratios measured for H_2, Ar, CH_4, and Xe by May *et al.* in 2007 over the temperature range (200 to 400) K, reducing the uncertainties of the data to 0.055%, 0.038%, 0.067%, and 0.084%, respectively. Separately, we extend the technique of combining viscosity ratios with *ab initio* calculations to develop new reference correlations for the dilute gas viscosity of 10 gases: helium, neon, argon, krypton, xenon, hydrogen, nitrogen, methane, ethane, and propane. This is achieved by combining the ratios of viscosities calculated *ab initio* at the target temperature and at 298.15 K with experimentally-based reference viscosity values for each gas at 298.15 K. The new reference dilute gas viscosity correlations span temperature ranges from at least (150 to 1200) K, with relative uncertainties between 30% (krypton) to 85% (methane) lower than the original *ab initio* results. For the noble gases, *ab initio* calculations for the Prandtl number are used to develop reference correlations for thermal conductivity ranging from at least (100 to 5000) K, with relative uncertainties ranging from 0.04% (argon) to 0.20% (xenon). The new reference correlations are compared with available experimental data at dilute gas conditions. In general, the data agree with the new correlations within the claimed experimental uncertainty.

Key words: reference correlations; viscosity; thermal conductivity; dilute gas; helium; neon; argon; krypton; xenon; methane; nitrogen; hydrogen; ethane; propane

Contents

Abstract 1

1. Introduction 4
2. Updated Experimental Transport Properties for H_2, CH_4, Ar, and Xe 5
3. Reference Correlations for the Dilute Gas Transport Properties of Ten Fluids 9
4. Reference Correlation Uncertainty 19
5. Results and Discussion 21
6. Conclusions 34

Supplementary Material 34

Acknowledgements 34

7. References 35

List of Tables

Table 1. Reference viscosities, η, for 11 gases (at 298.15 K and zero density) and their standard uncertainties $u(\eta)$ from Berg and Moldover.[30] 6

Table 2. Transport properties of argon at zero density, plus values at a finite pressure p = 100 kPa, re-evaluated from the viscosity ratio measurements of May *et al.*[4] 7

Table 3. Transport properties of xenon at zero density, plus values at a finite pressure p = 100 kPa, re-evaluated from the viscosity ratio measurements of May *et al.*[4] 7

Table 4. Viscosities of methane at zero density, plus values at a finite pressure p = 100 kPa, re-evaluated from the viscosity ratio measurements of May *et al.*[4] 8

Table 5. Viscosities of hydrogen at zero density, plus values at a finite pressure p = 100 kPa, re-evaluated from the viscosity ratio measurements of May *et al.*[4] 8

Table 6. List of the authors, temperature ranges, and the relative uncertainties in the viscosity, $u_r(\eta)$ and thermal conductivity, $u_r(\lambda)$, calculated from the corresponding *ab initio* potential. 10

Table 7. Values of the parameters a_i used in the functions $r_\eta^{\mathrm{gas}}(T)$ defined in Eq. (3) to represent the *ab initio* viscosity ratios. 12

Table 8. Values of the parameters b_i used in the functions $r_\lambda^{\mathrm{gas}}(T)$ defined in Eq. (4) to represent the *ab initio* thermal conductivity ratios. 12

Table 9. Values of $\eta_{T_0}^{\mathrm{gas}}$ and $\lambda_{T_0}^{\mathrm{gas}}$ with their estimated relative uncertainties together with other intermolecular potentials for noble gases used for the uncertainty estimates. 16

Table 10. Average (r.m.s) relative uncertainties for $r_\eta^{\mathrm{gas}}(T)$, $r_\lambda^{\mathrm{gas}}(T)$, $\eta_{\mathrm{ref}}^{\mathrm{gas}}(T)$, and $\lambda_{\mathrm{ref}}^{\mathrm{gas}}(T)$ over the temperature range of each reference correlation 20

Table 11. Summary of literature sources for experimental dilute gas transport properties.....21

List of Figures

FIG 1. ***a*** *Ab initio* viscosity ratios $r_\eta^{\mathrm{gas}}(T)$ from Eq. (3) for five noble gases as a function of temperature. ***b*** *Ab initio* viscosity ratios $r_\eta^{\mathrm{gas}}(T)$ from Eq. (3) for helium and four non-noble gases as a function of temperature. ***c*** *Ab initio* thermal conductivity ratios $r_\lambda^{\mathrm{gas}}(T)$ from Eq. (4) for five noble gases as a function of temperature. ***d*** Fractional differences between $r_\eta^{\mathrm{gas}}(T)_{\mathrm{AI}}$ and $r_\lambda^{\mathrm{gas}}(T)_{\mathrm{AI}}$ as a function of temperature. 11

FIG. 2 The fractional residuals of the ratios $r_\eta^{\mathrm{gas}}(T)_{\mathrm{AI}}$ from the best-fit correlating functions $r_\eta^{\mathrm{gas}}(T)$. 14

FIG. 3 The fractional residuals of the ratios $r_\lambda^{\mathrm{gas}}(T)_{\mathrm{AI}}$ from the best-fit correlating functions $r_\lambda^{\mathrm{gas}}(T)$. 15

FIG. 4 Absolute dilute gas viscosity and thermal conductivity reference values calculated from Eqs. (5) and (6). ***a*** Reference dilute gas viscosity correlations for five noble gases. ***b*** Reference dilute gas viscosity correlation for helium and four non-noble gases. ***c*** Reference dilute gas thermal conductivity correlations for helium, neon, and argon. ***d*** Reference dilute gas thermal conductivity correlations for krypton and xenon. 17

FIG. 5 Relative deviations of the reference dilute gas viscosities and thermal conductivities from the values calculated *ab initio*. ***a*** Dilute gas viscosity deviations for five noble gases. ***b*** Dilute gas viscosity deviations for four non-noble gases. ***c*** Dilute gas thermal conductivity deviations for five noble gases.....18

FIG. 6 ***a*** and ***b*** Viscosity deviations for helium. ***c*** Thermal conductivity deviation for helium. 25

FIG. 7 ***a*** Viscosity deviations for neon. ***b*** Thermal conductivity deviations for neon.....26

FIG. 8 ***a*** and ***b*** Viscosity deviations for argon. ***c*** Thermal conductivity deviations for argon.28

FIG. 9 ***a*** and ***b*** Viscosity deviations for krypton. ***c*** Thermal conductivity deviations for krypton. 29

FIG. 10 ***a*** and ***b*** Viscosity deviations for xenon. ***c*** Thermal conductivity deviations for xenon. 31

FIG. 11 Viscosity deviations for methane. 32

FIG. 12 Viscosity deviations for hydrogen. 32

FIG. 13 Viscosity deviations for nitrogen 33

FIG. 14 Viscosity deviations for propane. 33

1. Introduction

Dilute gas transport properties serve as a basis for predicting transport properties at high pressures and are important for calibrating scientific apparatus and other measurement devices.[1, 2] For example, accurate viscosities are crucial for the calibration of certain low-flow meters for mass spectrometers,[3, 4] and precise thermal conductivities at low densities are required for acoustic thermometry, determination of the universal gas constant,[5, 6] and were important to recent (and final) measurements of the Boltzmann constant prior to its re-definition.[7]

Several experimental methods are available for measuring viscosities accurately under low density conditions, including rotating-body viscometers,[8-10] oscillating-disk viscometers[11-14] and capillary viscometers.[3, 4, 15] With these apparatus, relative uncertainties in the order of 0.1% of the fluid viscosity are possible for temperatures from (200 to 700) K (all the uncertainties mentioned in this work are standard uncertainties corresponding to a coverage factor of k=1).

Theoretical methods of determining dilute gas properties based on *ab initio* calculations have become increasingly important as these can access even wider ranges of temperature at significantly lower cost. State-of-the-art *ab initio* potentials allow robust estimates of transport properties in the limit of zero density. Key advantages of such calculations are the extremely wide range of accessible temperatures (e.g., 83 K to 10000 K for argon[16]); uncertainties in absolute viscosity and thermal conductivity that, for helium, are nearly two orders of magnitude smaller than any existing experimental measurements; and for noble gases the ability to determine thermal conductivity from viscosity because the relative uncertainty in the *ab initio* Prandtl number is around 4×10^{-5}.[17]

One limitation of *ab initio* results is that the derived properties in the literature are typically only given in tabulated form at discrete temperatures, whereas applications often require transport properties at arbitrary temperatures. This drawback can be overcome by regressing *ab initio* derived data to empirical functions of temperature. A pertinent example is the recent work on the viscosity of dilute methane by Laesecke and Muzny.[18-20] Motivated by the approximate solution of the Boltzmann equation from Chapman and Enskog[21] for a monatomic gas, their formulation was developed via symbolic regression involving functions of $T^{1/6}$.

More importantly, *ab initio* results are typically of larger uncertainty than experimental measurements for all gases except helium,[16, 22-29] which still restricts the potential application of these theoretical achievements. Here we show how this issue can be solved by the application of viscosity ratios. Reference values for the viscosity of up to 11 gases can be anchored to the viscosity of helium calculated *ab initio* via the use of experimental viscosity ratios as applied

by Berg and Moldover.[30] Next these reference values are combined with the ratio of two dilute gas viscosities calculated *ab initio* at the temperature of interest and at 298.15 K. This eliminates the offset normally present in the absolute viscosity calculated *ab initio* due to uncertainties in the pair potential for that fluid, while retaining the wide temperature range covered by the calculations. To generalise this approach to all temperatures within the range of the calculations, empirical interpolating functions for the *ab initio* calculated viscosity ratios were developed based on an approach similar to Laesecke and Muzny.[18-20]

Compared to viscosity, thermal conductivity is far more difficult to measure accurately, particularly for dilute gases.[2] Assael *et al.*[31] used a transient hot-wire instrument to measure the thermal conductivity of several noble gases with an estimated accuracy of 0.20% at 308.15 K and pressures as low as 0.5 MPa. At the lower pressures relevant to dilute gas conditions, accurate measurements of thermal conductivity become extremely challenging. However, at least for noble gases, comparable or even smaller uncertainties can be obtained from direct *ab initio* calculations of the thermal conductivity.[16, 22, 26, 28, 32] By combining ratios of *ab initio* thermal conductivities with both a Prandtl number calculated *ab initio* and a reference viscosity ratio linking the noble gas to helium, the smallest uncertainty is achieved.

This work presents reference equations for the dilute gas viscosity of helium, neon, argon, krypton, xenon, methane, hydrogen, nitrogen, and propane from at least (150 to 1200) K. Reference equations for the dilute gas thermal conductivity of the noble gases (helium, neon, argon, krypton, and xenon) are also developed. The reference equations have equal (only for helium) or lower (for other gases) uncertainty than the values calculated *ab initio* from which they were in large part derived. A critical assessment of the available experimental data for dilute gas transport properties, including updated values of the measurements reported by May *et al.*,[4] is presented over wide ranges of temperature via comparison with the reference correlations.

2. Updated Experimental Transport Properties for H_2, CH_4, Ar, and Xe

Before developing the reference correlations, we first report updated values of the dilute gas transport properties measured for four gases by May *et al.*[4] over the temperature range (200 to 400) K. At each temperature, by alternately flowing the target gas and then helium at identical conditions through a two-capillary viscometer, the ratio of the gas viscosities ($\eta_T^{\mathrm{gas}}/\eta_T^{\mathrm{He}}$) was determined. This was then converted into a dilute gas viscosity for the target gas by combining the measured ratio with (i) a reference viscosity $\eta_{T_0}^{\mathrm{He}}$ for helium at 298.15 K, (ii) a reference ratio ($\eta_{T_0}^{\mathrm{gas}}/\eta_{T_0}^{\mathrm{He}}$) for the viscosities of the target gas and helium at 298.15 K, and (iii) an *ab initio* calculation of the ratio of helium's viscosity at the experimental temperature to that at 298.15 K, $(\eta_T^{\mathrm{He}}/\eta_{T_0}^{\mathrm{He}})_{\mathrm{AI}}$. (Here and throughout this paper the following notation is used: η_T^{gas} denotes a dilute gas viscosity for the gas indicated in the superscript and at the temperature T; and the reference temperature of 298.15 K is denoted by T_0. To denote a gas viscosity at a finite pressure, an additional subscript p is used, e.g., $\eta_{T,p}^{\mathrm{gas}}$. To indicate dilute gas transport property values calculated *ab initio*, or the ratio of two such values, an additional subscript "AI" is used).

The measurements of May *et al.*[4] were published five years prior to the *ab initio* values for helium reported by Cencek *et al.*[32] and the reference gas viscosity ratios recommended by Berg and Moldover.[30] Thus the source of the gas viscosity ratio at 298.15 K needed for (ii) was a

measurement made using a single quartz capillary viscometer, while the older *ab initio* calculations of Hurly and Mehl[33] were used to determine the ratio of helium's viscosities at various temperatures needed for (iii). At the time, the values of $\eta_{T_0}^{\mathrm{He}}$ calculated *ab initio* and measured using the single-capillary viscometer differed by more than twice their combined uncertainties. Consequently, an intermediate reference value was used with an increased uncertainty that spanned both values. The uncertainties of the temperature-dependent viscosity values η_T^{gas} reported for hydrogen, methane, argon, and xenon were dominated by this increased uncertainty resulting from the discrepancy that existed at the time between theory and experiment.

The subsequent improvements in the accuracy of the *ab initio* calculations for helium's dilute gas transport properties present an opportunity to reanalyze the data of May *et al.*[4] to reduce their uncertainty and provide a more stringent test of reference correlations for transport properties. Most significantly, by using the reference value for $\eta_{T_0}^{\mathrm{He}}$ of Cencek *et al.*[32] the uncertainty in the data of May *et al.*[4] is reduced by factors between 1.3 and 2.2 for each of the four gases. The improved *ab initio* potential of Cencek *et al.*[32] also reduces the contribution to the uncertainty of $(\eta_T^{\mathrm{He}}/\eta_{T_0}^{\mathrm{He}})_{\mathrm{AI}}$ to a negligible level. Furthermore, the review and critical assessment of the viscosity ratios $(\eta_{T_0}^{\mathrm{gas}}/\eta_{T_0}^{\mathrm{He}})$ by Berg and Moldover[30] obtained over multiple experiments for each of the four gases further increases the confidence in the reanalyzed data of May *et al.*[4] The values of $(\eta_{T_0}^{\mathrm{gas}}/\eta_{T_0}^{\mathrm{He}})$ used by May *et al.*[4] were consistent with the recommended ratios of Berg and Moldover[30] within their combined uncertainties. Table 1 lists the reference dilute gas viscosities $\eta_{T_0}^{\mathrm{gas}}$ recommended for eleven gases by Berg and Moldover[30] together with the reference ratios $(\eta_{T_0}^{\mathrm{gas}}/\eta_{T_0}^{\mathrm{He}})$ and their associated uncertainties. These were also used to estimate the uncertainties of the reanalyzed temperature-dependent dilute gas viscosities from May *et al.*[4] which are listed in Table 2 to Table 5 for argon, xenon, methane, and hydrogen, respectively.

Table 1. Reference viscosities, η, for 11 gases (at 298.15 K and zero density) and their standard uncertainties $u(\eta)$ from Berg and Moldover.[30] The helium value is from the *ab initio* calculation of Cencek *et al.*,[32] while the reference values for the other gases were calculated from experimental viscosity ratios combined with the *ab initio* helium value. The ratio of each dilute gas viscosity relative to that of helium and the uncertainties of that ratio are also listed.

Gas	$\eta_{T_0}^{\mathrm{gas}}$/(μPa s)	$u(\eta)$/(μPa s)	$(\eta_{T_0}^{\mathrm{gas}}/\eta_{T_0}^{\mathrm{He}})$	$u(\eta_{T_0}^{\mathrm{gas}}/\eta_{T_0}^{\mathrm{He}})$
Helium	19.8253	0.0002	1	
Neon	31.7088	0.0100	1.5994	0.0005
Argon	22.5666	0.0060	1.1383	0.0003
Krypton	25.3062	0.0080	1.2765	0.0004
Xenon	23.0183	0.0072	1.1611	0.0004
Methane	11.0631	0.0035	0.5580	0.0002
Nitrogen	17.7494	0.0048	0.8953	0.0002
Hydrogen	8.8997	0.0030	0.4489	0.0002
Propane	8.1399	0.0028	0.4106	0.0001
Sulfur hexafluoride	15.2234	0.0054	0.7679	0.0003
Ethane	9.2305	0.0030	0.4656	0.0002

For argon and xenon, May *et al.*[4] used the potentials of Boyes[34] and Dham *et al.*,[35] respectively, to calculate the dilute gas thermal conductivity λ_T^{gas} of these monatomic gases at the temperature of the viscosity measurements. For noble gases, the predicted value of the ratio $(\lambda_T^{\mathrm{gas}}/\eta_T^{\mathrm{gas}})$ is insensitive to the choice of the potential and it makes a negligible contribution to the uncertainty of the thermal conductivity derived from the measured viscosity. For this work, the more recent and accurate *ab initio* potentials of Vogel *et al.*[16] and Hellmann *et al.*[28] were used to calculate the values of $(\lambda_T^{\mathrm{gas}}/\eta_T^{\mathrm{gas}})$ for argon and xenon, respectively, when re-evaluating the values of λ_T^{gas} for these fluids derived from the viscosity data of May *et al.*,[4] which are also listed in Table 2 and Table 3.

Table 2. Transport properties of argon at zero density, plus values at a finite pressure p = 100 kPa, re-evaluated from the viscosity ratio measurements of May *et al.*[4] The re-evaluated transport properties and ratios listed have a standard relative uncertainty of 0.038%.

T / K	$(\eta_T^{\mathrm{Ar}}/\eta_T^{\mathrm{He}})$	η_T^{Ar} / μPa s	$\eta_{T,p}^{\mathrm{Ar}}$ / μPa s	λ_T^{Ar} / mW m^{-1} K^{-1}
202.71	1.05231	16.0657	16.0907	12.5422
210.75	1.06227	16.6476	16.6717	12.9970
213.19	1.06538	16.8260	16.8499	13.1365
223.66	1.07726	17.5724	17.5951	13.7201
230.29	1.08429	18.0393	18.0613	14.0852
248.14	1.10140	19.2730	19.2934	15.0504
248.25	1.10153	19.2810	19.3014	15.0567
273.15	1.12171	20.9502	20.9686	16.3631
298.14	1.13818	22.5643	22.5811	17.6270
298.14	1.13806	22.5620	22.5787	17.6252
298.15	1.13827	22.5666	22.5834	17.6288
298.15	1.13825	22.5662	22.5830	17.6285
298.15	1.13819	22.5650	22.5818	17.6276
315.33	1.14774	23.6423	23.6580	18.4715
330.48	1.15517	24.5726	24.5875	19.2006
335.96	1.15772	24.9062	24.9208	19.4621
351.08	1.16379	25.8053	25.8192	20.1671
371.45	1.17113	26.9959	27.0089	21.1009
391.56	1.17723	28.1418	28.1541	21.9996
391.57	1.17728	28.1435	28.1558	22.0009
394.20	1.17807	28.2930	28.3051	22.1181

Table 3. Transport properties of xenon at zero density, plus values at a finite pressure p = 100 kPa, re-evaluated from the viscosity ratio measurements of May *et al.*[4] The re-evaluated transport properties and ratios listed have a standard relative uncertainty of 0.084%.

T / K	$(\eta_T^{\mathrm{Xe}}/\eta_T^{\mathrm{He}})$	η_T^{Xe} / μPa s	$\eta_{T,p}^{\mathrm{Xe}}$ / μPa s	λ_T^{Xe} / mW m^{-1} K^{-1}
202.882	1.03554	15.8186	15.8186	3.7569
213.014	1.05067	16.5846	16.5865	3.9387
227.454	1.07205	17.6871	17.6922	4.2005
246.053	1.09775	19.0995	19.1093	4.5359
275.557	1.13513	21.3276	21.3460	5.0650

298.147	1.16111	23.0192	23.0450	5.4668
298.149	1.16093	23.0157	23.0415	5.4660

Table 4. Viscosities of methane at zero density, plus values at a finite pressure p = 100 kPa, re-evaluated from the viscosity ratio measurements of May *et al.*[4] The re-evaluated viscosities and viscosity ratios listed have a standard relative uncertainty of 0.067%.

T / K	$(\eta_T^{CH_4}/\eta_T^{He})$	$\eta_T^{CH_4}$ / μPa s	$\eta_{T,p}^{CH_4}$ /μPa s
210.756	0.51478	8.0676	8.0806
225.810	0.52442	8.6097	8.6227
248.251	0.53676	9.3954	9.4084
273.157	0.54837	10.2420	10.2540
298.145	0.55807	11.0638	11.0748
298.149	0.55795	11.0615	11.0735
298.151	0.55806	11.0637	11.0747
313.223	0.56309	11.5461	11.5571
331.550	0.56856	12.1213	12.1323
352.568	0.57398	12.7641	12.7751
371.193	0.57808	13.3190	13.3290
391.543	0.58204	13.9133	13.9223
391.551	0.58204	13.9135	13.9225

Table 5. Viscosities of hydrogen at zero density, plus values at a finite pressure p = 100 kPa, re-evaluated from the viscosity ratio measurements of May *et al.*[4] The re-evaluated viscosities and viscosity ratios listed have a standard relative uncertainty of 0.055%.

T / K	$(\eta_T^{H_2}/\eta_T^{He})$	$\eta_T^{H_2}$ / μPa s	$\eta_{T,p}^{H_2}$ /μPa s
213.615	0.44691	7.0677	7.0697
227.744	0.44746	7.3886	7.3906
241.269	0.44786	7.6893	7.6913
255.544	0.44822	8.0010	8.0020
269.369	0.44852	8.2979	8.2989
278.805	0.44864	8.4968	8.4978
283.570	0.44878	8.5981	8.6001
298.129	0.44902	8.9015	8.9025
298.142	0.44892	8.8997	8.9007
313.223	0.44919	9.2105	9.2115
332.201	0.44940	9.5936	9.5936
354.974	0.44954	10.0437	10.0447
374.388	0.44964	10.4211	10.4211
374.396	0.44962	10.4208	10.4208
394.209	0.44969	10.8000	10.8000

In addition to the dilute gas transport properties listed in Tables 2-5, values are listed for the viscosity $\eta_{T,p}^{\mathrm{gas}}$ of each gas at a finite pressure of p = 100 kPa. The methods used for estimating the initial density dependence of each fluid's transport properties were the same as those used by May *et al.*[4]

3. Reference Correlations for the Dilute Gas Transport Properties of Ten Fluids

The second objective of this work was to develop continuously-defined reference correlations for the dilute gas viscosities and thermal conductivities of multiple fluids, which have an uncertainty comparable to that of the reference viscosity ratios at 298.15 K recommended by Berg and Moldover.[30] This was done for 10 of the 11 gases analyzed by Berg and Moldover,[30] with SF_6 omitted because we could not find any reliable *ab initio* calculations of its transport properties. For the 10 other fluids, the first step towards our second objective was to define the quantities $r_\eta^{\mathrm{gas}}(T)_{\mathrm{AI}}$ and $r_\lambda^{\mathrm{gas}}(T)_{\mathrm{AI}}$ using Eqs. (1) and (2).

$$r_\eta^{\mathrm{gas}}(T)_{\mathrm{AI}} \equiv \left(\frac{(\eta_T^{\mathrm{gas}})_{\mathrm{AI}}}{(\eta_{T_0}^{\mathrm{gas}})_{\mathrm{AI}}}\right), \qquad (1)$$

$$r_\lambda^{\mathrm{gas}}(T)_{\mathrm{AI}} \equiv \left(\frac{(\lambda_T^{\mathrm{gas}})_{\mathrm{AI}}}{(\lambda_{T_0}^{\mathrm{gas}})_{\mathrm{AI}}}\right). \qquad (2)$$

These quantities are simply the ratio of the transport property calculated *ab initio* using a particular pair potential at the target temperature T to the value calculated at the reference temperature, T_0 = 298.15 K. The *ab initio* pair potentials used to calculate $r_\eta^{\mathrm{gas}}(T)_{\mathrm{AI}}$ and $r_\lambda^{\mathrm{gas}}(T)_{\mathrm{AI}}$ for each of the ten fluids are listed in Table 6. In each case, values of $r_\eta^{\mathrm{gas}}(T)_{\mathrm{AI}}$ and $r_\lambda^{\mathrm{gas}}(T)_{\mathrm{AI}}$ are only calculated at discrete temperatures, at a spacing chosen by authors of the potentials to ensure that no significant loss of accuracy occurs upon a linear interpolation between any two temperatures.

Table 6. List of the authors, temperature ranges, and the relative uncertainties in the viscosity, $u_r(\eta)$ and thermal conductivity, $u_r(\lambda)$, calculated from the corresponding *ab initio* potential.

Gas	Authors	Temperature Ranges /K	$10^2\, u_r(\eta)$	$10^2\, u_r(\lambda)$
Helium	Cencek *et al.*[32]	1 to 10000	0.001	0.001
Neon	Bich *et al.*[22, 23]	25 to 10000	0.1	0.1
Argon	Vogel *et al.*[16]	83.81 to 10000	0.1	0.1[b]
Krypton	Jäger *et al.*[26]	70 to 5000	0.13	0.13
Xenon	Hellmann *et al.*[28]	100 to 5000	0.14	0.14
Methane	Hellmann *et al.*[36]	80 to 1500	1[a]	
Nitrogen	Hellmann[25]	70 to 3000	0.5[b]	
Hydrogen	Mehl *et al.*[29]	20 to 2000	0.08[c] 1[b,d]	
Ethane	Hellmann[37]	90 to 1200	0.15[e] 0.5[f]	
Propane	Hellmann[27]	150 to 1200	2[g] 1[h]	

a) The viscosity values calculated *ab initio* were re-scaled to match experimental results but no further uncertainty estimate was provided.[38] The uncertainty value here is taken from the original paper.

b) The uncertainty was not mentioned in the publication and was estimated in this work based on comparisons with experimental measurements and other theoretical calculations.

c) For 200 K < T < 400 K;

d) For other temperatures;

e) For 250 K < T < 700 K;

f) For other temperatures;

g) For 150 K <T <250 K and 700 K< T < 1200 K;

h) For 250 K < T < 700 K.

Continuously defined correlating functions $r_\eta^{\mathrm{gas}}(T)$ and $r_\lambda^{\mathrm{gas}}(T)$ were then developed in this work by regressing the discrete sets of $r_\eta^{\mathrm{gas}}(T)_{\mathrm{AI}}$ and $r_\lambda^{\mathrm{gas}}(T)_{\mathrm{AI}}$ available for each gas to the following equations.

$$r_\eta^{\mathrm{gas}}(T) = \exp\left(\sum_{i=1}^{N} a_i [\ln\left(\frac{T}{T_0}\right)]^i\right), \quad (3)$$

$$r_\lambda^{\mathrm{gas}}(T) = \exp\left(\sum_{i=1}^{n} b_i (\ln\left(\frac{T}{T_0}\right))^i\right). \quad (4)$$

The choice of these functions was based upon polynomial forms that are of a sufficiently precise and smooth representation of the $r_\eta^{\mathrm{gas}}(T)_{\mathrm{AI}}$ and $r_\lambda^{\mathrm{gas}}(T)_{\mathrm{AI}}$ values with the number of adjustable parameters being kept to as few as possible. The number of terms and parameters used for each gas and property varied, in part according to the temperature range covered by the *ab initio* calculations. The values of the parameters a_i and b_i used for each gas are listed in Table 7 and Table 8, respectively: the number of significant figures shown for each parameter is the minimum required to achieve the stated accuracy obtained in the fit. Figure 1 illustrates the fitted r values over the various temperature ranges for which they are defined for different gases.

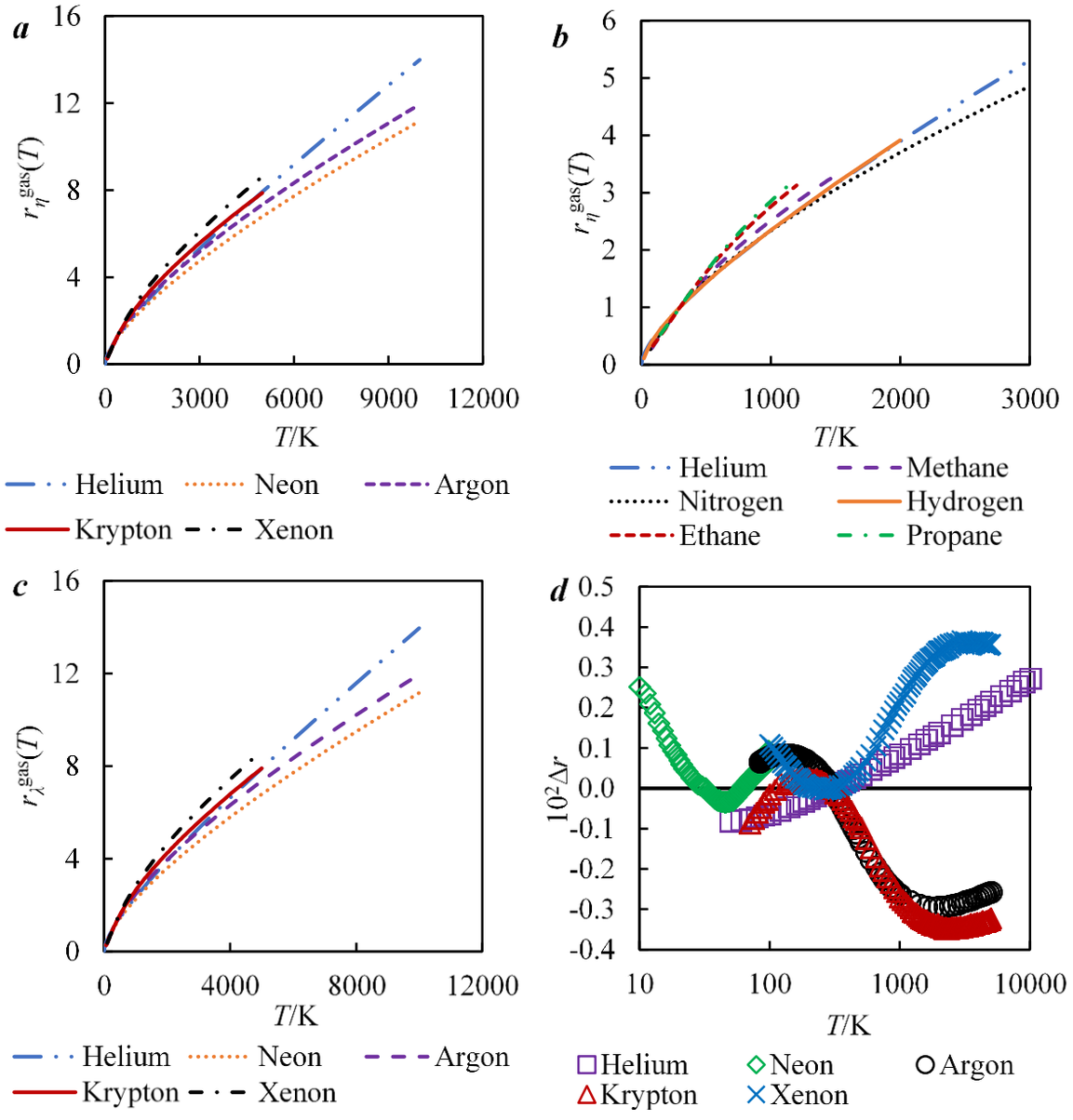

FIG 1. ***a*** *Ab initio* viscosity ratios $r_\eta^{\mathrm{gas}}(T)$ from Eq. (3) for five noble gases as a function of temperature. ***b*** *Ab initio* viscosity ratios $r_\eta^{\mathrm{gas}}(T)$ from Eq. (3) for helium and four non-noble gases as a function of temperature. $r_\eta^{\mathrm{He}}(T)$ is exhibited in part a and part b for the purpose of comparison: the temperature range plotted in each case reflects the domain over which the *ab initio* transport properties were calculated. ***c*** *Ab initio* thermal conductivity ratios $r_\lambda^{\mathrm{gas}}(T)$ from Eq. (4) for five noble gases as a function of temperature. ***d*** Fractional differences between $r_\eta^{\mathrm{gas}}(T)_{\mathrm{AI}}$ and $r_\lambda^{\mathrm{gas}}(T)_{\mathrm{AI}}$ as a function of temperature, $\Delta r \equiv (r_\eta^{\mathrm{gas}}(T)_{\mathrm{AI}} - r_\lambda^{\mathrm{gas}}(T)_{\mathrm{AI}})/\, r_\eta^{\mathrm{gas}}(T)_{\mathrm{AI}}$. The curves for helium and krypton in ***a*** and ***c***, and for hydrogen and helium in ***b*** are indistinguishable at the scale of the figure.

The similarity of the curves in Fig. 1*a* and Fig. 1*c* for each gas reflects the link between viscosity and thermal conductivity for monatomic gases established through first-order kinetic theory. However, although very similar, the noble gas $r_\eta^{\mathrm{gas}}(T)$ and $r_\lambda^{\mathrm{gas}}(T)$ functions are not identical because the *ab initio* calculations upon which they were based utilized up to fifth-order approximations of the kinetic theory. The relative differences between the noble gas viscosity and thermal conductivity ratio functions are up to 0.4% in magnitude as shown in Fig.

1*d*. The differences are also reflected in Table 7 and Table 8 where the coefficients a_i and b_i for each noble gas are similar but not identical.

Table 7. Values of the parameters a_i used in the functions $r_\eta^{\text{gas}}(T)$ defined in Eq. (3) to represent the *ab initio* viscosity ratios.

	Helium	Neon	Argon	Krypton	Xenon
a_1	6.8257552×10^{-1}	6.75404×10^{-1}	8.395115×10^{-1}	9.129712×10^{-1}	9.652514×10^{-1}
a_2	1.4496203×10^{-2}	-2.03522×10^{-2}	-1.062564×10^{-1}	-1.001470×10^{-1}	-5.237199×10^{-2}
a_3	1.1987706×10^{-3}	1.61102×10^{-2}	1.065796×10^{-2}	-2.454742×10^{-2}	-6.758414×10^{-2}
a_4	$-6.7722412 \times 10^{-5}$	-4.88074×10^{-3}	1.879809×10^{-2}	3.145009×10^{-2}	2.855787×10^{-2}
a_5	4.9875650×10^{-5}	5.32334×10^{-4}	-8.881774×10^{-3}	-4.456257×10^{-3}	1.002789×10^{-2}
a_6	$-6.1456994 \times 10^{-6}$	2.93695×10^{-4}	-9.613779×10^{-5}	-4.511243×10^{-3}	-9.639621×10^{-3}
a_7	1.3189407×10^{-6}	-1.55155×10^{-4}	1.404406×10^{-3}	2.237544×10^{-3}	1.329770×10^{-3}
a_8	$-3.7245774 \times 10^{-7}$	3.10797×10^{-5}	-4.321739×10^{-4}	-1.455422×10^{-4}	1.114305×10^{-3}
a_9	1.3671981×10^{-8}	-2.50504×10^{-6}	-2.544782×10^{-5}	-2.006385×10^{-4}	-5.992234×10^{-4}
a_{10}	5.0354149×10^{-8}	2.74563×10^{-8}	4.398471×10^{-5}	8.341288×10^{-5}	1.224218×10^{-4}
a_{11}	$-1.5714379 \times 10^{-8}$		-9.997908×10^{-6}	-1.520236×10^{-5}	-9.584978×10^{-6}
a_{12}	1.4720785×10^{-9}		7.753453×10^{-7}	1.159085×10^{-6}	
	Methane	Nitrogen	Hydrogen	Ethane	Propane
a_1	8.73963×10^{-1}	7.734578×10^{-1}	6.91306×10^{-1}	9.6979×10^{-1}	9.61184×10^{-1}
a_2	-1.17213×10^{-1}	-9.310761×10^{-2}	2.66280×10^{-3}	-6.6974×10^{-2}	3.19607×10^{-3}
a_3	3.29256×10^{-4}	2.716958×10^{-2}	8.54435×10^{-3}	-8.3319×10^{-2}	-1.04277×10^{-1}
a_4	2.65091×10^{-2}	6.175553×10^{-3}	-2.48813×10^{-3}	3.3060×10^{-2}	8.75362×10^{-3}
a_5	-9.11659×10^{-3}	-7.201594×10^{-3}	6.74482×10^{-4}	1.6154×10^{-2}	3.77555×10^{-2}
a_6	-1.65050×10^{-3}	2.094372×10^{-3}	-1.38186×10^{-5}	-8.5036×10^{-3}	-2.07079×10^{-2}
a_7	1.78886×10^{-3}	1.922676×10^{-4}	-4.18999×10^{-5}	-6.9635×10^{-4}	-3.93610×10^{-3}
a_8	-3.38860×10^{-4}	-3.454323×10^{-4}	6.70026×10^{-6}	3.6971×10^{-4}	1.01132×10^{-2}
a_9		1.051771×10^{-4}			-3.42913×10^{-3}
a_{10}		-1.126739×10^{-5}			

Table 8. Values of the parameters b_i used in the functions $r_\lambda^{\text{gas}}(T)$ defined in Eq. (4) to represent the *ab initio* thermal conductivity ratios.

	Helium	Neon	Argon	Krypton	Xenon
b_1	6.8192175×10^{-1}	6.76478×10^{-1}	8.417395×10^{-1}	9.141101×10^{-1}	9.65524×10^{-1}
b_2	1.4441872×10^{-2}	-2.13734×10^{-2}	-1.050326×10^{-1}	-9.862299×10^{-2}	-5.12353×10^{-2}
b_3	1.2138429×10^{-3}	1.63523×10^{-2}	9.711009×10^{-3}	-2.413946×10^{-2}	-6.70913×10^{-2}
b_4	$-7.4912205 \times 10^{-5}$	-4.79402×10^{-3}	1.816630×10^{-2}	3.072989×10^{-2}	2.88938×10^{-2}
b_5	5.2123986×10^{-5}	4.23959×10^{-4}	-8.386976×10^{-3}	-5.044719×10^{-3}	9.25546×10^{-3}
b_6	$-6.0795764 \times 10^{-6}$	3.35013×10^{-4}	4.444459×10^{-5}	-4.048633×10^{-3}	-9.72175×10^{-3}
b_7	8.6135146×10^{-7}	-1.53714×10^{-4}	1.190663×10^{-3}	2.383010×10^{-3}	1.69364×10^{-3}
b_8	$-2.6311453 \times 10^{-7}$	2.45053×10^{-5}	-3.875653×10^{-4}	-3.046862×10^{-4}	9.96803×10^{-4}
b_9	6.8367328×10^{-8}	-5.03701×10^{-7}	1.257878×10^{-6}	-1.901802×10^{-4}	-6.10466×10^{-4}
b_{10}	1.6608814×10^{-8}	-1.67000×10^{-7}	2.592767×10^{-5}	1.008519×10^{-4}	1.33327×10^{-4}
b_{11}	$-9.0525341 \times 10^{-9}$		-5.736442×10^{-6}	-2.014480×10^{-5}	-1.09858×10^{-5}
b_{12}	$9.9986305 \times 10^{-10}$		3.974198×10^{-7}	1.544358×10^{-6}	

Figures 2 and 3 show the fractional residuals of the ratios $r_\eta^{\text{gas}}(T)_{\text{AI}}$ and $r_\lambda^{\text{gas}}(T)_{\text{AI}}$ from the best-fit correlating functions $r_\eta^{\text{gas}}(T)$ and $r_\lambda^{\text{gas}}(T)$. The correlations were regressed to represent the $r_\eta^{\text{gas}}(T)_{\text{AI}}$ and $r_\lambda^{\text{gas}}(T)_{\text{AI}}$ values listed in the original publication to at least one order of magnitude smaller than their uncertainty, with the majority of the correlations able to represent *ab initio* dilute gas transport properties to the same precision originally reported. By doing so, the functions representing $r_\eta^{\text{gas}}(T)$ and $r_\lambda^{\text{gas}}(T)$ potentially may not need to be re-fit when more

accurate pair potentials are available, and/or the uncertainties (as opposed to the precisions) of the $r_\eta^{\mathrm{gas}}(T)_{\mathrm{AI}}$ and $r_\lambda^{\mathrm{gas}}(T)_{\mathrm{AI}}$ are improved. For argon, the *ab initio* tranport properties used to develop the correlating functions $r_\eta^{\mathrm{Ar}}(T)_{\mathrm{AI}}$ and $r_\lambda^{\mathrm{Ar}}(T)_{\mathrm{AI}}$ were first updated[39] to a higher degree of numerical precision than given in the original publication (T ranges from 83.8 K to 5000 K).

One limitation of the functional forms used in Eqs (3) and (4) to correlate the *ab initio* visosity and thermal conductivity ratios is they do not extrapolate as expected theoretically, particularly at low temperatures. Laesecke and Muzny[18-20] used symbollic regression to determine a functional form to correlate the viscosity of methane calculated *ab initio* that remains finite when extraoplated well beyond the *ab initio* data to which it was fit, all the way to a temperature of absolute zero. However, the functional form and limited number of parameters in the correlation of Laesecke and Muzny[18-20] means it is unable to represent the *ab initio* methane viscosity data to within their numerical precision (as opposed to their uncertainty). Accordingly, in the Supplementary Information, we present an alternative set of viscosity and thermal conductivity ratio correlations based on a Gaussian functional form that behave as expected theoretically over the range (0 to 10000) K, even when extrapolated well beyond the data to which they were fit. For a given fluid, these alternative correlating functions have more parameters than those used in polynomial functions shown in Eqs (3) and (4) but still do not quite achieve the same level of precision. A comparison of the extrapolative behaviour and the numerical precision of the two sets of correlation functions is presented in the SI. In practice, the two sets are largely equivalent in performance: we suggest use of the polynomial functions for calculations that remain within the temperature range over which the founding *ab initio* data were generated.

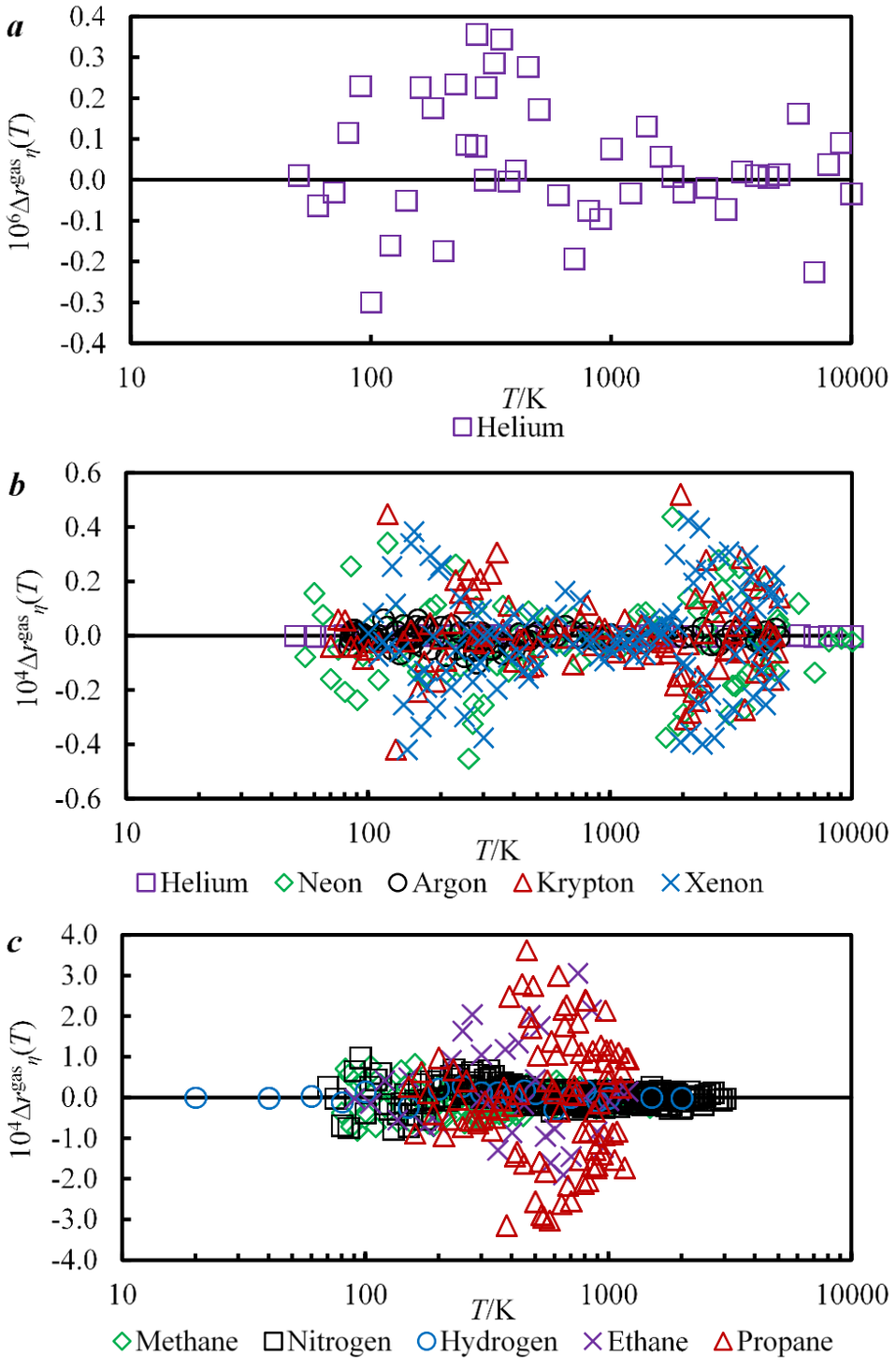

FIG. 2 The fractional residuals of the ratios $r_\eta^{\mathrm{gas}}(T)_{\mathrm{AI}}$ from the best-fit correlating functions $r_\eta^{\mathrm{gas}}(T)$. Helium was set apart due to the higher precision of the *ab initio* values. The minimum temperature regressed in the correlations is 50 K (20 K for hydrogen). $\Delta r_\eta^{\mathrm{gas}}(T)=(r_\eta^{\mathrm{gas}}(T)_{\mathrm{AI}}-r_\eta^{\mathrm{gas}}(T))/r_\eta^{\mathrm{gas}}(T)$.

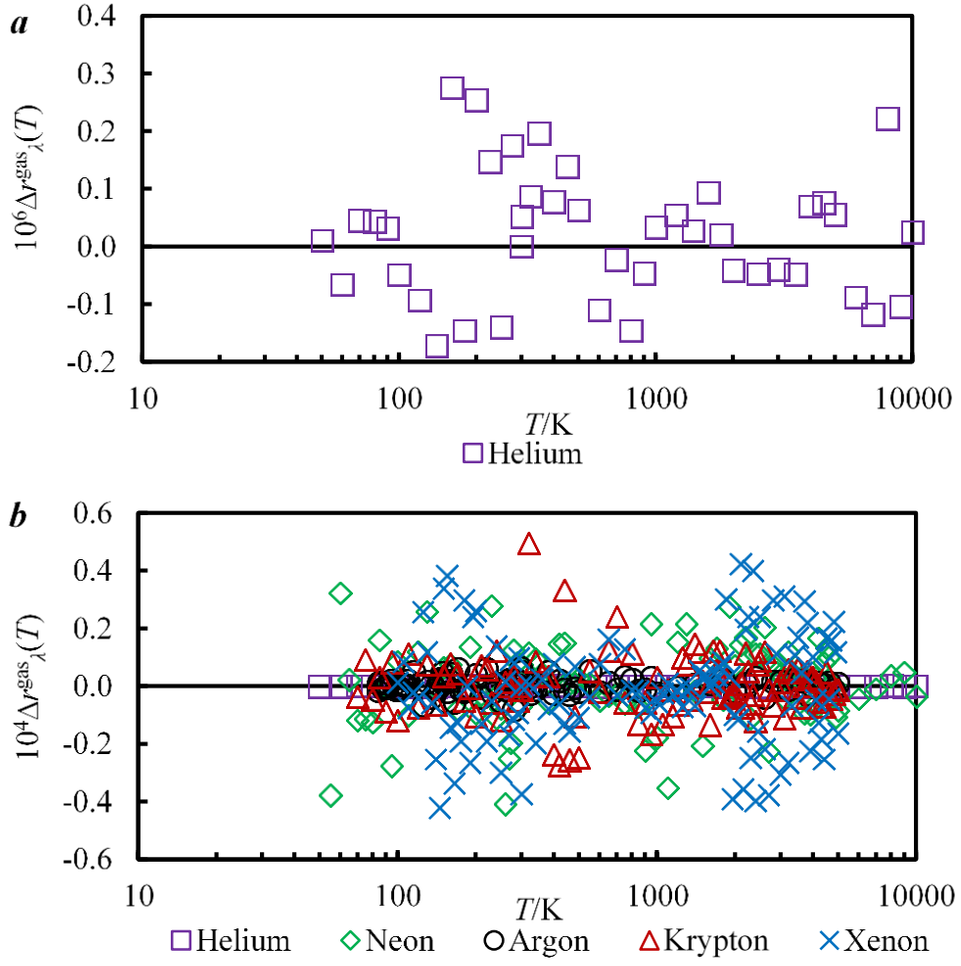

FIG. 3 The fractional residuals of the ratios $r_\lambda^{\mathrm{gas}}(T)_{\mathrm{AI}}$ from the best-fit correlating functions $r_\lambda^{\mathrm{gas}}(T)$. Helium was set apart due to the higher precision of the *ab initio* values. The minimum temperature regressed in the correlations is 50 K. $\Delta r_\lambda^{\mathrm{gas}}(T) = (r_\lambda^{\mathrm{gas}}(T)_{\mathrm{AI}} - r_\lambda^{\mathrm{gas}}(T))/r_\lambda^{\mathrm{gas}}(T)$.

The wide-ranging reference correlations for the dilute gas transport properties are then simply

$$\eta_{\mathrm{ref}}^{\mathrm{gas}}(T) = r_\eta^{\mathrm{gas}}(T) \times \left(\frac{\eta_{T_0}^{\mathrm{gas}}}{\eta_{T_0}^{\mathrm{He}}}\right) \times \eta_{T_0}^{\mathrm{He}} \quad = \quad r_\eta^{\mathrm{gas}}(T) \times \eta_{T_0}^{\mathrm{gas}}, \tag{5}$$

$$\lambda_{\mathrm{ref}}^{\mathrm{gas}}(T) = r_\lambda^{\mathrm{gas}}(T) \times \left(\frac{\lambda_{T_0}^{\mathrm{gas}}}{\eta_{T_0}^{\mathrm{gas}}}\right) \times \left(\frac{\eta_{T_0}^{\mathrm{gas}}}{\eta_{T_0}^{\mathrm{He}}}\right) \times \eta_{T_0}^{\mathrm{He}} \quad = \quad r_\lambda^{\mathrm{gas}}(T) \times \lambda_{T_0}^{\mathrm{gas}}. \tag{6}$$

In Eqs (5) and (6), $\eta_{T_0}^{\mathrm{He}}$ is the reference viscosity of helium at 298.15 K calculated *ab initio* by Cencek *et al.*,[32] $(\eta_{T_0}^{\mathrm{gas}}/\eta_{T_0}^{\mathrm{He}})$ is the reference viscosity ratio at 298.15 K derived from experiments and recommended by Berg and Moldover, and $\eta_{T_0}^{\mathrm{gas}}$ is the reference viscosity for the gas at 298.15 K obtained from the product of the former two quantities; for each gas, all three of these constant reference values are listed in Table 1. In Eq. (6), $(\lambda_{T_0}^{\mathrm{gas}}/\eta_{T_0}^{\mathrm{gas}})$ is the ratio of the thermal conductivity to viscosity at 298.15 K calculated *ab initio* for the monatomic gas, and $\lambda_{T_0}^{\mathrm{gas}}$ is the reference thermal conductivity of the dilute monatomic gas at 298.15 K, obtained from the product of the former *ab initio* ratio with the reference dilute gas viscosity $\eta_{T_0}^{\mathrm{gas}}$ listed in Table

1. The uncertainties of $\eta_{T_0}^{\mathrm{gas}}$ and $\lambda_{T_0}^{\mathrm{gas}}$ are estimated from thr uncertainty of $\eta_{T_0}^{\mathrm{He}}$ from Cencek *et al.*, the reference viscosity recommended by Berg and Moldover and, for thermal conductivity, the ratio of ($\lambda_{T_0}^{\mathrm{gas}}/\eta_{T_0}^{\mathrm{gas}}$); the uncertainty of this last quantity is estimated via comparison with values of the ratio calculated via other intermolecular potentials, as described originally by May *et al.*[17] and discussed further below. The values of $\eta_{T_0}^{\mathrm{gas}}$ and $\lambda_{T_0}^{\mathrm{gas}}$ used in this work, together with the intermolecular potentials used to calculate their estimated uncertainties, are listed in Table 9.

Table 9. Values of $\eta_{T_0}^{\mathrm{gas}}$ and $\lambda_{T_0}^{\mathrm{gas}}$ with their estimated relative uncertainties together with other intermolecular potentials for noble gases used for the uncertainty estimates.

Gas	$\eta_{T_0}^{\mathrm{gas}}$ /μPa s	$\lambda_{T_0}^{\mathrm{gas}}$ / mW m^{-1} K^{-1}	$10^2 u_{\mathrm{r}}(\eta_{T_0}^{\mathrm{gas}})$	$10^2 u_{\mathrm{r}}(\lambda_{T_0}^{\mathrm{gas}})$	Other intermolecular potentials used to evaluate $u_{\mathrm{r}}(\lambda_{T_0}^{\mathrm{gas}})$
Helium	19.8253	155.0008	0.0001	0.001	Hurly and Moldover,[40] Hurly and Mehl,[33] Bich *et al.*[41]
Neon	31.7088	49.1732	0.031	0.031	Slaman and Aziz[42]
Argon	22.5666	17.6286	0.027	0.038	Patkowski *et al.*,[43] Boyes,[34] Aziz[44]
Krypton	25.3062	9.4183	0.032	0.032	Aziz and Slaman,[45] Waldrop *et al.*[46]
Xenon	23.0183	5.4666	0.031	0.040	Dham *et al.*[35]
Methane	11.0631		0.031		
Nitrogen	17.7494		0.027		
Hydrogen	8.8997		0.034		
Ethane	9.2305		0.033		
Propane	8.1399		0.035		

Figure 4 shows the reference correlations for dilute gas viscosity plotted for all ten fluids and the reference correlations for dilute gas thermal conductivity for noble gases over the temperature range for which they are defined. Figure 5 exhibits the fractional deviations for the (discrete set of) *ab initio* viscosities calculated for each gas from $\eta_{\mathrm{ref}}^{\mathrm{gas}}(T)$ and the corresponding fractional deviations of the *ab initio* thermal conductivities calculated for each gas from $\lambda_{\mathrm{ref}}^{\mathrm{gas}}(T)$. The patterns in the deviations are similar to those observed for ratio correlating functions $r_{\eta}^{\mathrm{gas}}(T)$ and $r_{\lambda}^{\mathrm{gas}}(T)$ except for a fluid-specific offset: this corresponds to the difference between the value of $\eta_{T_0}^{\mathrm{gas}}$ calculated directly from the *ab initio* potential and the recommended value obtained from the helium reference value $\eta_{T_0}^{\mathrm{He}}$ of Cencek *et al.*[32] and the

experimentally-based reference viscosity ratio recommended by Berg and Moldover.[30] By using the $\eta_{T_0}^{\text{gas}}$ obtained from experimental viscosity ratios combined with the theoretically-derived reference viscosity for helium in conjunction with the continuously defined ratio correlating functions, it is possible to produce wide-ranging reference correlations for dilute gas transport properties for multiple fluids with uncertainties that are (i) much smaller than previously achieved, and (ii) comparable with the remarkably small uncertainties achieved for helium.

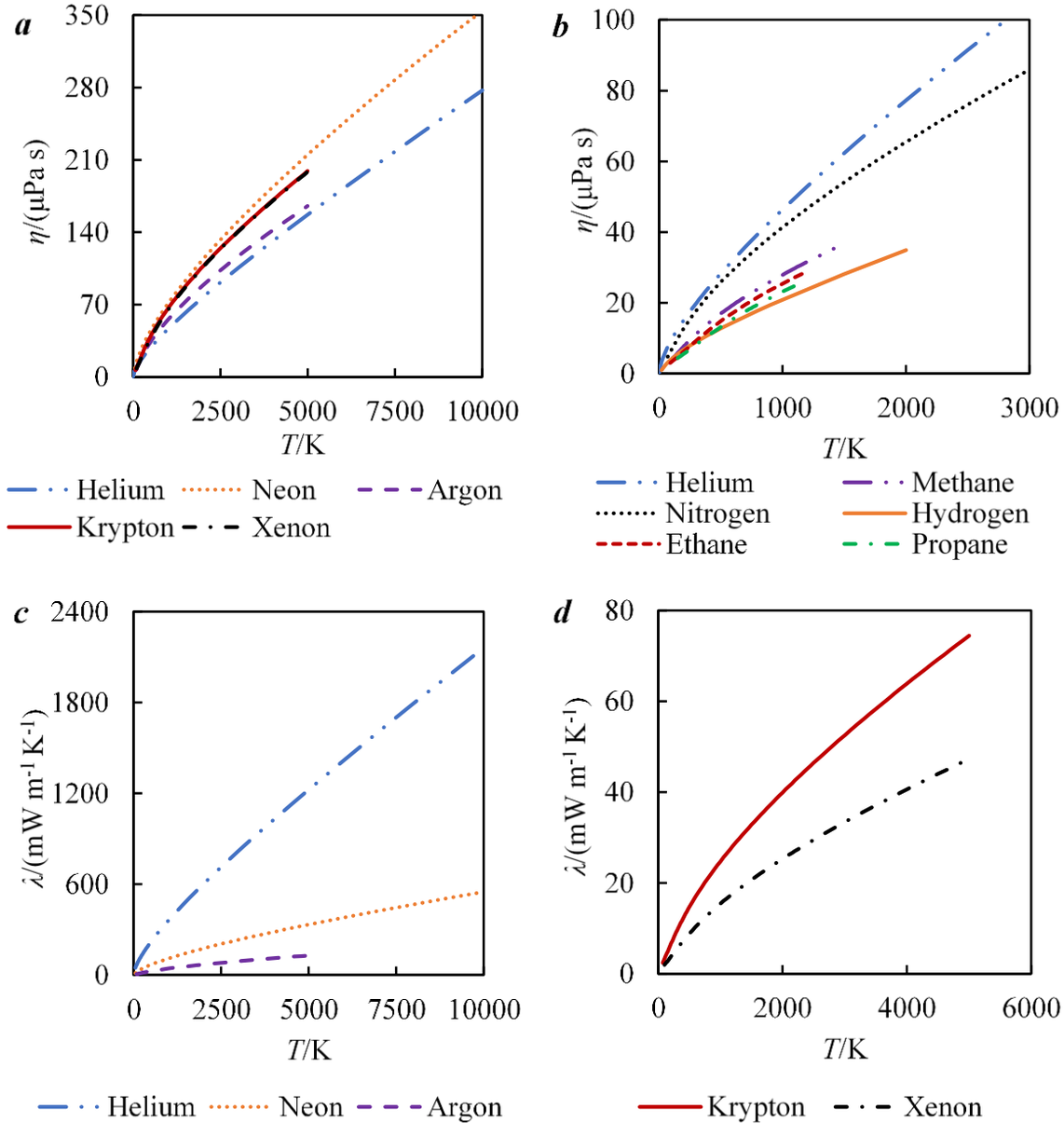

FIG. 4 Absolute dilute gas viscosity and thermal conductivity reference values calculated from Eqs. (5) and (6). ***a*** Reference dilute gas viscosity correlations for five noble gases. ***b*** Reference dilute gas viscosity correlation for helium and four non-noble gases. $(\eta_T^{\text{He}})_{\text{ref}}$ is shown in both plots for comparison. ***c*** Reference dilute gas thermal conductivity correlations for helium, neon, and argon. ***d*** Reference dilute gas thermal conductivity correlations for krypton and xenon. The curves in ***a*** for krypton and xenon are indistinguishable at the scale of the figure.

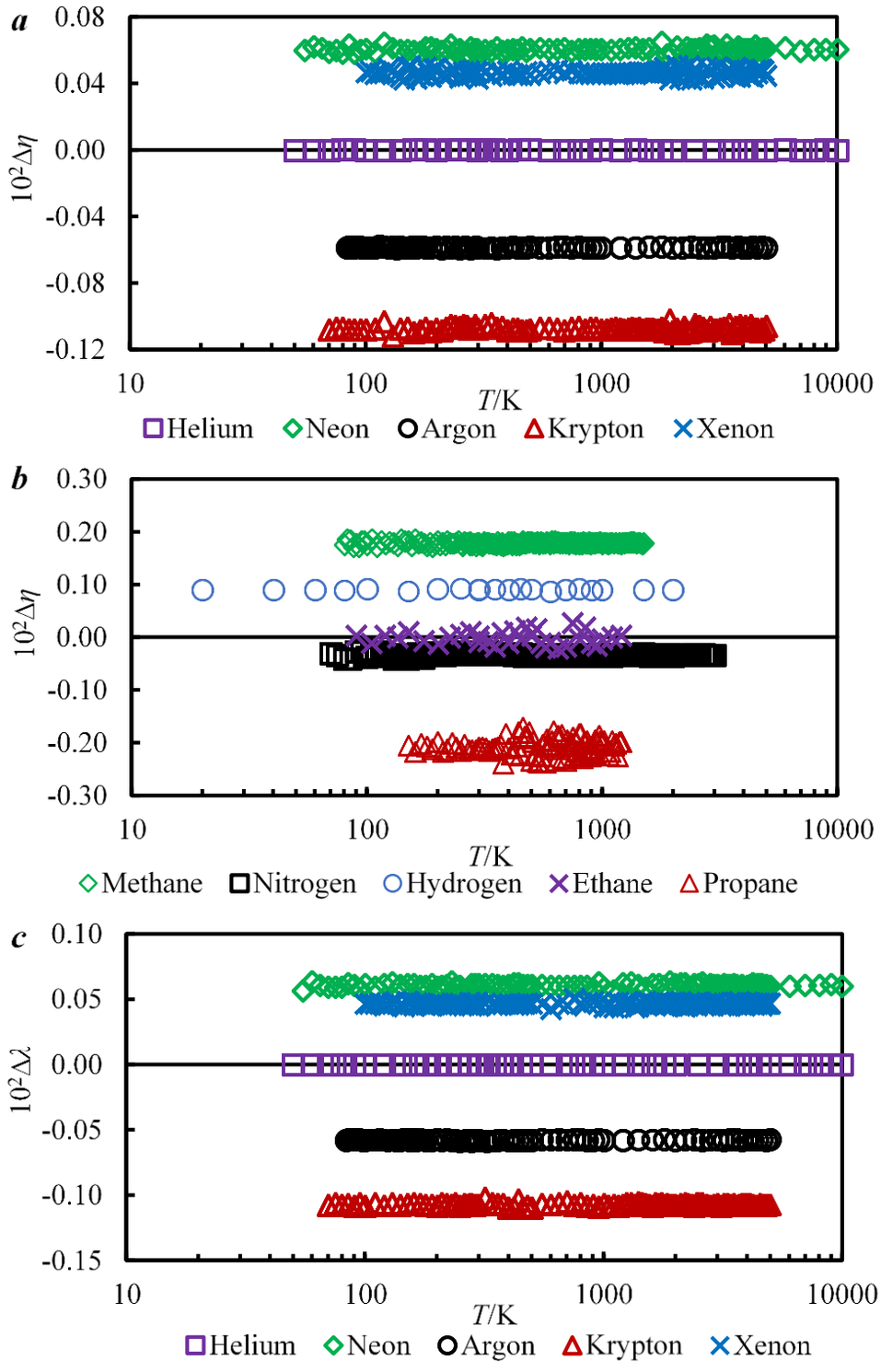

FIG. 5 Relative deviations of the reference dilute gas viscosities and thermal conductivities from the values calculated *ab initio*. $\Delta\eta = ((\eta_T^{\mathrm{gas}})_{\mathrm{AI}} - \eta_{\mathrm{ref}}^{\mathrm{gas}}(T))/\eta_{\mathrm{ref}}^{\mathrm{gas}}(T)$; $\Delta\lambda = ((\lambda_T^{\mathrm{gas}})_{\mathrm{AI}} - \lambda_{\mathrm{ref}}^{\mathrm{gas}}(T))/\lambda_{\mathrm{ref}}^{\mathrm{gas}}(T)$. ***a*** Dilute gas viscosity deviations for five noble gases. ***b*** Dilute gas viscosity deviations for four non-noble gases. ***c*** Dilute gas thermal conductivity deviations for five noble gases.

For most gases, the effect of re-scaling in this work can be seen in Fig. 5 where the *ab initio* results are offset from the reference equation. For krypton, methane, and propane, the offsets are large and significant improvements were achieved. For ethane, the reference correlation is based entirely on the *ab initio* calculated values because the difference between the viscosity data from the most recent intermolecular potential for ethane[37] and the recommended viscosity from Berg and Moldover at 298.15 K is smaller than their combined uncertainties. For other gases, the differences tend to be small (i.e. less than 0.10%). Nonetheless, considering the uncertainty of the high-quality experimental data are 0.10% for viscosity and 0.20% for thermal conductivity, such shifts of the *ab initio* calculations are not negligible. As a result of these offsets, the experimental data available for most gases have smaller deviations from the reference correlations than from the original *ab initio* results (see Section 5). The inherent uncertainties of the reference correlations are smaller than those of the values calculated *ab initio*, as discussed below and shown in Table 10.

4. Reference Correlation Uncertainty

There are two primary contributions to the uncertainty of the reference correlations: that due to the reference value at 298.15 K, and that of the ratio correlating functions. The former is generally well defined and given by Berg and Moldover:[30] with the exception of helium, the relative standard uncertainty in $\eta_{T_0}^{\mathrm{gas}}$ for all gases ranges from (0.027 to 0.035) %. The relative standard uncertainty of the $\lambda_{T_0}^{\mathrm{gas}}$ for argon, xenon, and krypton is 0.027%, 0.031%, and 0.032%, respectively. The uncertainty contribution due to the ratio correlating functions $r_\eta^{\mathrm{gas}}(T)$ and $r_\lambda^{\mathrm{gas}}(T)$ is set by the quality of the fits of Eqs. (3) and (4) to the $r_\eta^{\mathrm{gas}}(T)_{\mathrm{AI}}$ and $r_\lambda^{\mathrm{gas}}(T)_{\mathrm{AI}}$ values, and the uncertainty of the *ab initio* ratios to which the correlations were fit. The contribution introduced by the fits is negligible and hence the primary task of the uncertainty analysis becomes the estimation of the uncertainty in $r_\eta^{\mathrm{gas}}(T)_{\mathrm{AI}}$ and $r_\lambda^{\mathrm{gas}}(T)_{\mathrm{AI}}$.

The uncertainty of the ratio of two transport properties at different temperatures calculated *ab initio* is smaller than that of each calculated value because the errors common to the calculation of both will cancel when the ratio is evaluated. To estimate the uncertainties in $r_\eta^{\mathrm{gas}}(T)_{\mathrm{AI}}$ and $r_\lambda^{\mathrm{gas}}(T)_{\mathrm{AI}}$, we adapted the approach used by May *et al.*[17] to estimate the fractional uncertainty of an *ab initio* calculation of the Prandtl number for dilute argon at 200 K. Figure 8 of Ref. 17 shows the values of argon's Prandtl number calculated using six different pair potentials: hard sphere, Lennard-Jones, and four accurate potentials from the literature. The fractional uncertainty in the value of argon's dilute gas Prandtl number at 200 K was estimated to be 4×10^{-5} based on the maximum difference between values calculated using the four accurate potentials. In this work, we considered the variation in $r_\eta^{\mathrm{gas}}(T)_{\mathrm{AI}}$ produced when the constituent $\eta_{T,\mathrm{AI}}^{\mathrm{gas}}$ were derived from different potentials.,[33-35, 39-55] and/or experimental data at dilute gas conditions[14, 56-59] when a sufficient number of suitably accurate potentials were not available. At each temperature the uncertainty, $u(r_\eta^{\mathrm{gas}}(T)_{\mathrm{AI}})$ was taken to be the root mean square (r.m.s) deviation of the ratios determined from the available alternative sources. The same approach was also applied to evaluate the uncertainty, $u(r_\lambda^{\mathrm{gas}}(T)_{\mathrm{AI}})$, and the resulting uncertainties are shown as a function of temperature in the Supplementary Information. To

evaluate the uncertainties summarized in Table 10, an r.m.s. value over all temperatures was calculated.

The uncertainties for $\eta_{\rm ref}^{\rm gas}(T)$ or $\lambda_{\rm ref}^{\rm gas}(T)$ can be calculated by combining the uncertainties of $r_\eta^{\rm gas}(T)$ and $\eta_{T_0}^{\rm gas}$ or $r_\lambda^{\rm gas}(T)$ and $\lambda_{T_0}^{\rm gas}$, with $r_\eta^{\rm gas}(T)$ and $r_\lambda^{\rm gas}(T)$ being the dominant contributions. These estimates of the reference correlation uncertainties are tested subsequently by comparisons with the available experimental literature data for each fluid in Section 5. In most cases, however, the experimental uncertainties are too large for a stringent test of the correlation. Exceptions to this include the revised data from May *et al.*,[4] which have had their uncertainty reduced by factors of between 1.3 and 2.2 (or, equivalently, a fractional change of between (23 and 55) %), and are up to 73% smaller than the uncertainties of the values calculated with the corresponding *ab initio* pair potentials listed in Table 6.

Table 10. Average (r.m.s) relative uncertainties for $r_\eta^{\rm gas}(T)$, $r_\lambda^{\rm gas}(T)$, $\eta_{\rm ref}^{\rm gas}(T)$, and $\lambda_{\rm ref}^{\rm gas}(T)$ over the temperature range of each reference correlation plus the sources used to estimate the uncertainty.

Gas	$10^2 u_{\rm r}(r_\eta^{\rm gas}(T))$	$10^2 u_{\rm r}(r_\lambda^{\rm gas}(T))$	$10^2 u_{\rm r}(\eta_{\rm ref}^{\rm gas}(T))$	$10^2 u_{\rm r}(\lambda_{\rm ref}^{\rm gas}(T))$	Other sources
Helium	0.001	0.001	0.001	0.001	Hurly and Moldover,[40] Hurly and Mehl,[33] Bich *et al.*[41]
Neon	0.10	0.10	0.10	0.10	Slaman and Aziz[42], Cybulski and Toczyłowski[47]
Argon	0.05	0.05	0.06	0.06	Patkowski *et al.*,[43] Boyes[34] and Aziz[44]
Krypton	0.04	0.04	0.05	0.05	Aziz and Slaman,[45] Waldrop *et al.*[46]
Xenon	0.09	0.10	0.10	0.11	Dham *et al.*[35]
Methane	0.10	NA	0.10	NA	Zarkova *et al.*,[48] Nemati-Kande and Maghari[49]
Nitrogen	0.2	NA	0.2	NA	Jafari *et al.*,[50] Kestin *et al.*,[56] Vogel[14]
Hydrogen	0.04[a] 0.4[b]	NA	0.05[a] 0.4[b]	NA	Diep and Johnson,[51, 52] Wind and Røeggen,[53] Silvera and Goldman[54]
Ethane	0.15[c] 0.5[d]	NA	0.15[c] 0.5[d]	NA	Nemati-Kande and Maghari,[49] Vogel *et al.*[59]
Propane	0.8[e] 0.3[f]	NA	0.8[e] 0.3[f]	NA	Nemati-Kande and Maghari,[49] Vogel,[57] Kestin *et al.*[58]

a) For 200 K < T < 400 K;

b) For other temperatures;

c) For 250 K < T < 700 K;

d) For other temperatures;

e) For ethane, for 150 K < T < 250 K and 700 K < T < 1200 K;

f) For 250 K < T < 700 K

5. Results and Discussion

Deviation statistics between literature data from 64 sources and the reference equations developed in this work are shown in Table 11. The RMS deviations and the Bias for each property are calculated from Eq. (7) to Eq. (10), respectively.

$$\mathrm{RMS}(\eta) = \sqrt{\frac{1}{N}\sum\left(\frac{\eta_{\mathrm{exp}}^{\mathrm{gas}}(T)-\eta_{\mathrm{ref}}^{\mathrm{gas}}(T)}{\eta_{\mathrm{ref}}^{\mathrm{gas}}(T)}\right)^2}, \quad (7)$$

$$\mathrm{RMS}(\lambda) = \sqrt{\frac{1}{N}\sum\left(\frac{\lambda_{\mathrm{exp}}^{\mathrm{gas}}(T)-\lambda_{\mathrm{ref}}^{\mathrm{gas}}(T)}{\lambda_{\mathrm{ref}}^{\mathrm{gas}}(T)}\right)^2}, \quad (8)$$

$$\mathrm{Bias}(\eta) = \frac{1}{N}\sum\left(\frac{\eta_{\mathrm{exp}}^{\mathrm{gas}}(T)-\eta_{\mathrm{ref}}^{\mathrm{gas}}(T)}{\eta_{\mathrm{ref}}^{\mathrm{gas}}(T)}\right), \quad (9)$$

$$\mathrm{Bias}(\lambda) = \frac{1}{N}\sum\left(\frac{\lambda_{\mathrm{exp}}^{\mathrm{gas}}(T)-\lambda_{\mathrm{ref}}^{\mathrm{gas}}(T)}{\lambda_{\mathrm{ref}}^{\mathrm{gas}}(T)}\right). \quad (10)$$

Table 11. Summary of literature sources for experimental dilute gas transport properties.[a]

Authors	Uncertainty/%[b]	T/K	N[c,d]	RMS/%	Bias/%
Viscosities					
Helium					
Berg[60]	0.035	298.15	1	0.002	-0.002
Clarke and Smith[61]	1.0	77.45-343.90	10	0.70	0.62
Dawe *et al.*[62]	1.0	293.2-1600	15	1.44	-1.12
Gough *et al.*[63]	1.0	120-320	11	0.70	0.56
Kestin *et al.*[64]	0.2	298.15-678.15	8	0.33	0.30
Kestin *et al.*[65]	0.15	298.15-778.15	9	0.44	0.41
Maitland and Smith[66]	0.2	295-1533	11	1.29	-0.87
Seibt *et al.*[67]	0.30	293.15	1	0.29	-0.29
Tanaka *et al.*[68]	1.0	298.15-323.15	2	0.93	0.93
Vogel *et al.*[69]	0.3	294.46-647.92	20	0.11	0.10
Neon					
Clarke and Smith[61]	1.0	77.45-373.9	10	0.75	0.66
Dawe and Smith[70]	1.0	293.2-1600	15	1.39	-0.98
Edwards[71]	1.0	194.75-717.65	6	1.04	-0.82
Evers *et al.*[72]	0.15	298.15-348.15	2	0.06	0.04
Johnston and Grilly[73]	0.5	80-300	27	1.00	-0.88
Trautz and Zimmermann[74]	0.4	90-523	13	1.55	-1.42
Argon					
Clarke and Smith[75]	0.5	114.35-374.60	12	0.43	0.38
Dawe and Smith[70]	1.0	293.2-1600	15	0.76	-0.31

Gough *et al.*[63]	1.0	120-320	11	0.48	0.46
Hurly *et al.*[76]	0.36	293.15-373.15	4	0.15	0.14
Lin *et al.*[3]	0.062	298.15-653.15	14	0.08	-0.07
Maitland and Smith[77]	0.5	295-1533	11	0.61	-0.067
May *et al.*[4] [this work]	0.037	202.71-394.20	21	0.034	0.026
Vogel[12]	0.2	291.09-681.96	49	0.049	-0.040
Zhang *et al.*[78]	0.082	243.15-393.15	17	0.040	-0.032
Krypton					
Dawe and Smith[70]	1.0	293.2-1600	15	0.82	-0.30
Gough *et al.*[63]	1.0	120-320	11	0.48	0.47
Humberg and Richter[9]	0.13	253.20-473.37	8	0.11	0.10
Lin *et al.*[15]	0.10	243.15-393.15	17	0.14	0.13
Maitland and Smith[66]	0.5	295-1553	10	0.69	-0.26
Vogel[79]	0.2[e]	296.75-689.81	52	0.088	-0.019
	0.4[f]				
Wilhelm and Vogel[80]	0.2	298.15-348.15	2	0.22	0.22
Xenon					
Clarke and Smith[75]	0.5	176.0-374.6	9	0.33	0.28
Dawe and Smith[70]	1.0	293.2-1600	15	0.68	0.07
Lin *et al.*[15]	0.11	298.15-393.15	10	0.05	0.05
May *et al.*[4] [this work]	0.084	202.88-298.15	7	0.014	-7×10^{-5}
Rigby and Smith[81]	1.0	293-972	14	1.39	-1.09
Vogel[79]	0.2[g]	295.04-649.53	20	0.085	0.013
	0.4[h]				
Methane					
Dawe *et al.*[62]	1.0	293-1050	9	0.57	0.29
Gough *et al.* [63]	0.5	150-320	10	0.62	0.61
Humberg *et al.*[10]	0.25	253.16-473.17	9	0.09	-0.058
May *et al.*[4] [this work]	0.053	210.76-391.55	13	0.050	0.011
Meerlender and Aziz[82]	1.0	293.15-353.15	6	0.39	-0.36
Schley *et al.*[83]	0.3	260-360	6	0.042	0.025
Vogel[13]	0.2	289.05-682.14	35	0.20	0.18
Hydrogen					
Barua *et al.*[84]	0.15	223.15-423.15	6	0.42	-0.23
Gracki[85]	0.1	173.15-298.15	3	0.44	-0.41
Hongo and Iwasaki[86]	0.3	298.15-373.15	4	0.39	-0.026
May *et al.*[4] [this work]	0.020	213.62-394.21	15	0.016	0.014
Van Cleave and Maass[87]	1.0	89.75-295.15	2	0.54	-0.54
Nitrogen					
El Hawary[88]	0.25	253.16-473.17	7	0.52	0.47
Hoogland *et al.*[89]	0.1	298.11-333.10	5	0.11	0.098
Humberg *et al.*[8]	0.10	253.21-473.38	7	0.068	-0.064
Kestin *et al.*[56]	0.15	298.15-423.15	6	0.089	-0.003
Seibt *et al.*[90]	0.3	298.15-423.15	4	0.099	0.086
Seibt *et al.*[67]	0.3	293.18-423.11	2	0.34	-0.32
Trautz and Baumann[91]	1.0	195.15-523.25	19	1.08	-0.70
Vogel[14]	0.20	291.55-681.99	17	0.063	0.050
Ethane					
Iwasaki and Takahashi[92]	0.3	298.15-348.15	8	0.19	-0.13
Wilhelm *et al.*[93]	0.25	289.97-429.96	8	0.35	-0.34

Herrmann *et al.*[94]	0.3	289.83-675	19	0.054	-0.022
Propane					
Abe *et al.*[95]	0.3	298.15-468.15	5	0.70	0.60
Holland *et al.*[96]	1.0	140-500	18	0.77	0.48
Kestin *et al.*[58]	0.2	298.15-478.18	13	0.93	0.85
Seibt *et al.*[97]	0.3	273.18-366.10	3	0.93	-0.58
Vogel[57]	1.0	297.24-625.80	70	0.28	0.19
Wilhelm and Vogel[98]	0.4	298.21-423.09	7	0.24	-0.19
Thermal conductivities					
Helium					
Assael *et al.*[31]	0.22	308.15	1	0.22	0.22
Baker[99]	0.5	300-600	8	0.21	0.009
Kestin *et al.*[100]	0.3	300.65	1	0.55	0.55
Mukhopadhyay and Buarua[101]	1.0	90.18-473.25	6	0.47	-0.31
Mustafa *et al.*[102]	0.3	308.11-425.44	4	1.41	1.38
Neon					
De Groot *et al.*[103]	1.5	301.16	1	1.38	-1.38
Kestin *et al.*[100]	0.3	300.65	2	0.017	0.017
Keyes[104]	2.0	91.05-273.15	5	1.19	-1.17
Sengers *et al.*[105]	1.0	298.15-348.15	5	0.62	-0.60
Sevast'yanov and Zykov[106]	2.0	100-600	12	0.78	-0.67
Argon					
Assael *et al.*[31]	0.2	308.15	1	0.02	0.02
Haran *et al.*[107]	0.2	308.15-429.15	5	0.63	0.42
May *et al.*[4] [this work]	0.024	202.71-394.20	21	0.018	-0.004
Millat *et al.*[108]	0.3	308.15-428.15	3	0.80	0.70
Roder *et al.*[109]	1.0	339.24-339.82	19	0.38	0.37
Sun *et al.*[110]	1.0	297.89-403.18	36	0.39	-0.009
Krypton					
Assael *et al.*[31]	0.2	308.15	1	0.17	0.17
Vargaftik[111]	2.0	125-700	13	1.80	1.53
Voshchinin *et al.*[112]	2.0	591-976	7	1.78	1.27
Xenon					
Assael *et al.*[31]	0.30	308.15	1	0.069	0.069
Keyes[113]	NA	214.25-273.15	7	0.42	0.10
May *et al.*[4] [this work]	0.084	202.88-298.15	7	0.014	2×10^{-4}
Springer and Wingeier[114]	1.0	900-2500	9	0.70	-0.54

a) Literature data measured at low pressures were also included and were corrected to the dilute gas condition via Rainwater and Friend theory.[1]

b) The reported uncertainties sometimes change with temperature slightly. Under these circumstances the largest uncertainty is given in the table.

c) Some isothermal transport property data were reported at various pressures. In this case, only the lowest pressure point was corrected to the dilute gas condition for comparison.

d) The *N* value only includes the points fitted in this work. Data that are inconsistent with other reported measurements were not included.

e) For 295 K < *T* < 400 K;

f) For 400 K < T < 690 K;
g) For 295 K < T < 400 K;
h) For 400 K < T < 650 K

The sizes of most of the deviations are in fair agreement with the published estimates of the experimental uncertainty. Among the authors who have measured several different gases, a few have deviations that are smaller on average than their stated uncertainties (e.g., Clarke and Smith,[61] Dawe and Smith,[70] and Gough *et al.*[63]), while a few have deviations that are on average larger than their stated uncertainties (e.g., Kestin *et al.*[64, 100] and Mustafa *et al.*[102]).

The deviations between available experimental data and the reference equations for each fluid are shown in the following sections. Within the deviation figures, the 'ref' subscript refers to the reference values obtained from Eqs. (5) and (6), dot points refer to the experimental data, and the dashed curves refer to calculations made using the models implemented in the National Institute of Standards and Technology (NIST)'s developed software program REFPROP 10.[115]

For helium, since all the calculations in this work are based on the *ab initio* results, there is no shift in the reference correlation. Figure 6 shows a comparison of the *ab initio* calculated transport properties, available experimental data, and models implemented in REFPROP 10 relative to the reference correlation.

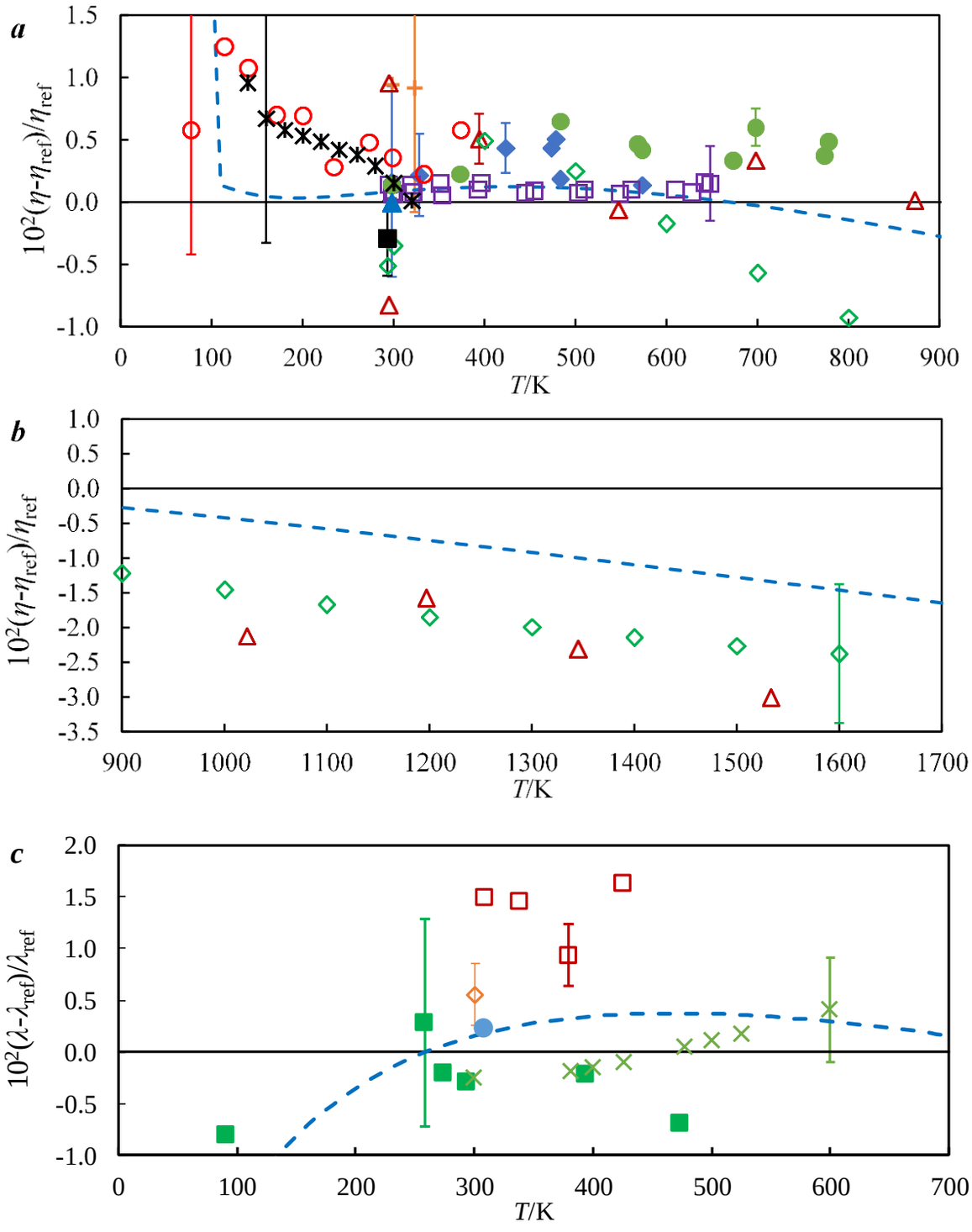

FIG. 6 ***a*** and ***b*** Viscosity deviations for helium. Experimental data: ▲, Berg;[60] ○, Clarke and Smith;[61] ◇, Dawe *et al.*;[62] ∗, Gough *et al.*;[63] ◆, Kestin *et al.*;[64] ●, Kestin *et al.*;[65] Δ, Maitland and Smith;[66] ■, Seibt *et al.*;[67] -, Tanaka *et al.*;[68] □, Vogel *et al.*[69] Blue long dash curve: model from Arp *et al.*[116] implemented in REFPROP 10. ***c*** Thermal conductivity deviation for helium. Experimental data: ▲, Assael *et al.*;[31] ×, Baker;[99] ◇, Kestin *et al.*;[100] □, Mustafa *et al.*;[102] ■, Mukhopadhyay and Barua.[101] Blue long dash curve: model from Hands and Arp[117] implemented in REFPROP 10.

Clarke and Smith[61] measured viscosities of helium, neon, and methane relative to that of nitrogen at 273.15 K. For all the plots, the original reported data are exhibited for comparison. These values could be further updated with the nitrogen viscosity value developed in this work, and for the helium viscosities, the RMS deviation would reduce from 0.68% to 0.37%. Maitland and Smith[66] and Dawe *et al.*[62] reported viscosity ratios of helium to nitrogen. However, as Berg and Moldover concluded,[30] helium is of higher accuracy than nitrogen in the reference correlations and should be used as the standard in the ratio measurements. For thermal conductivity, there are fewer available measurements. Differences between measured points and the reference correlation are generally larger than the differences observed for viscosities. Given the very small uncertainties in helium transport properties calculated *ab initio*, the accuracy claimed by Kestin *et al.*[64, 100] and Mustafa *et al.*[102] may be too optimistic. Models[116, 117] implemented in REFPROP 10 are of 10% uncertainty for both viscosity and thermal conductivity for all pressure conditions. From Fig. 6, the uncertainty for dilute gas helium is less than 1% at most temperatures.

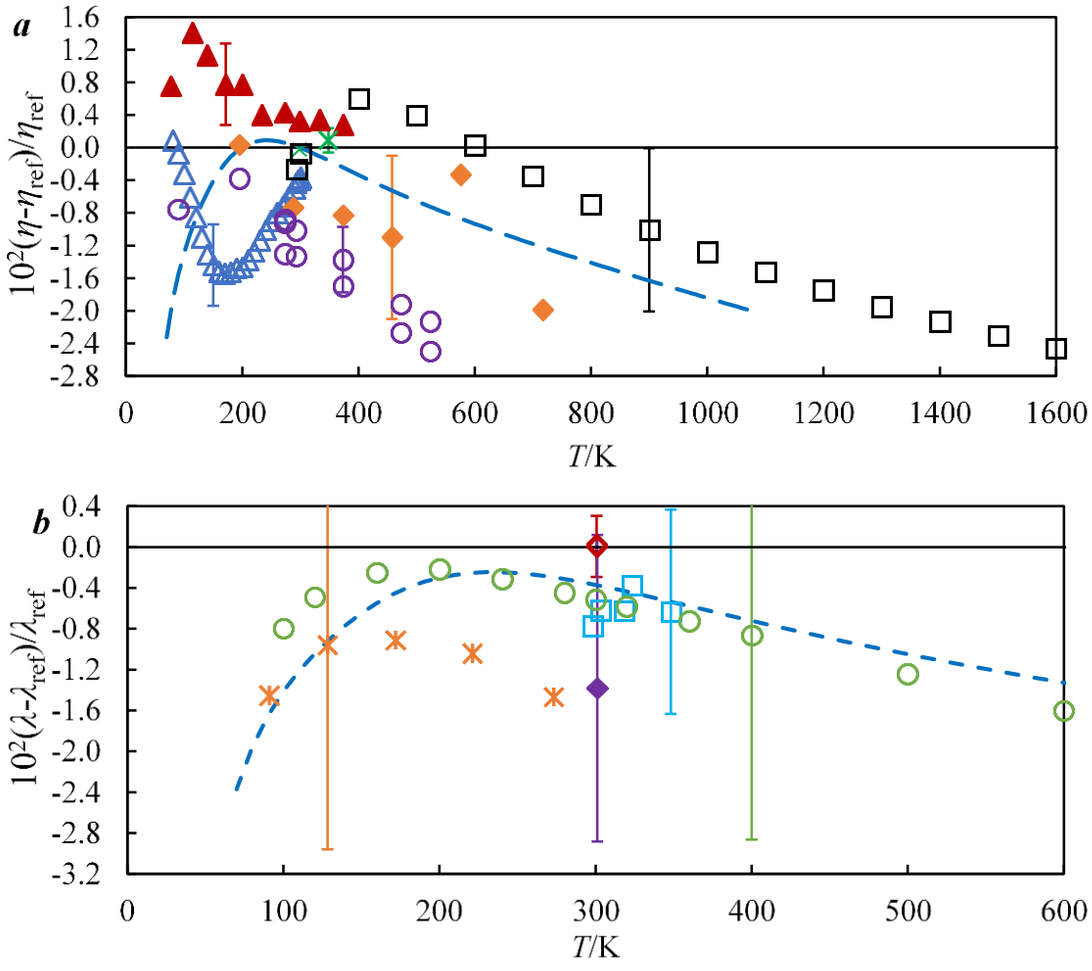

FIG. 7 ***a*** Viscosity deviations for neon. Experimental data: ▲, Clarke and Smith;[61] □, Dawe and Smith;[70] ◆, Edwards;[71] ×, Evers *et al.*;[72] △, Johnston and Grilly;[73] ○, Trautz and Zimmermann.[74] Blue long dash curve: model from Huber[118] implemented in REFPROP 10. ***b*** Thermal conductivity deviations for neon. Experimental data: ◆, De Groot *et al.*;[103] ◇, Kestin *et al.*;[100] ✳, Keyes;[104] □, Sengers *et al.*;[105] ○, Sevast'yanov and Zykov.[106] Blue long dash curve: model from Huber[118] implemented in REFPROP 10.

For neon, Clarke and Smith[61] reported the measured viscosity ratio of neon to nitrogen. The RMS deviation between the Clarke and Smith[61] viscosity values and the reference equation could be reduced from 0.78% to 0.45% if the former data were reanalyzed using the reference values for nitrogen calculated in this work. Most of the data from Johnston and Grilly,[73] Trautz and Zimmermann,[74] and Dawe and Smith[70] deviate negatively from the reference equation, and the deviation of the limited available data from the reference correlation increases in magnitude with temperature. For thermal conductivity, the data reported by Kestin *et al.*[100] have small uncertainties (0.3%) and are closer to the zero line (the reference correlation) than to the *ab initio* calculations (value of 0.061 in Fig. 7*b*). All the other data sources agree with each other within their relatively large uncertainty. Models[118, 119] implemented in REFPROP 10 were fitted to limited experimental data and have the highest uncertainties (3% for both viscosities and thermal conductivities). They exhibit the smallest deviations for some of the experimental data points (e.g., for the viscosities reported by Trautz and Zimmermann[74] and Johnston and Grilly[73]). Nevertheless, given the relatively high uncertainty of these experimental measurements and models, we recommend using the reference correlation for dilute neon viscosities and thermal conductivities.

For argon, there are many high-quality viscosity data and the reference correlation is within the experimental uncertainties. The data reported by Vogel[12] from an all-quartz oscillating-disk viscometer were calibrated based on the argon *ab initio* viscosity at 298.15 K, which explains why these points are even closer to the *ab initio* calculations than to the reference correlation. The data from Lin *et al.*[3] are very close to the results of May *et al.*[4] from (293.15 to 393.15) K, but at higher temperatures the data tend to deviate from the reference equation by more than their stated uncertainties. The reported data for the thermal conductivities of argon are of relatively large uncertainty. For most of the data, the deviations in Fig. 8*b* from the zero line are within the experimental uncertainties. There are several exceptions where the deviations are larger than the uncertainties. However, the deviations of the data from May *et al.*[4] and Assael *et al.*[31] are very small. The models of Lemmon and Jacobsen[119] implemented in REFPROP 10 have moderate uncertainties (0.5% for viscosity and 2% for thermal conductivity) but do not quite agree with high quality data sets (May *et al.*,[4] Vogel,[12] Lin *et al.*,[3] and Assael *et al.*[31]) within these uncertainties.

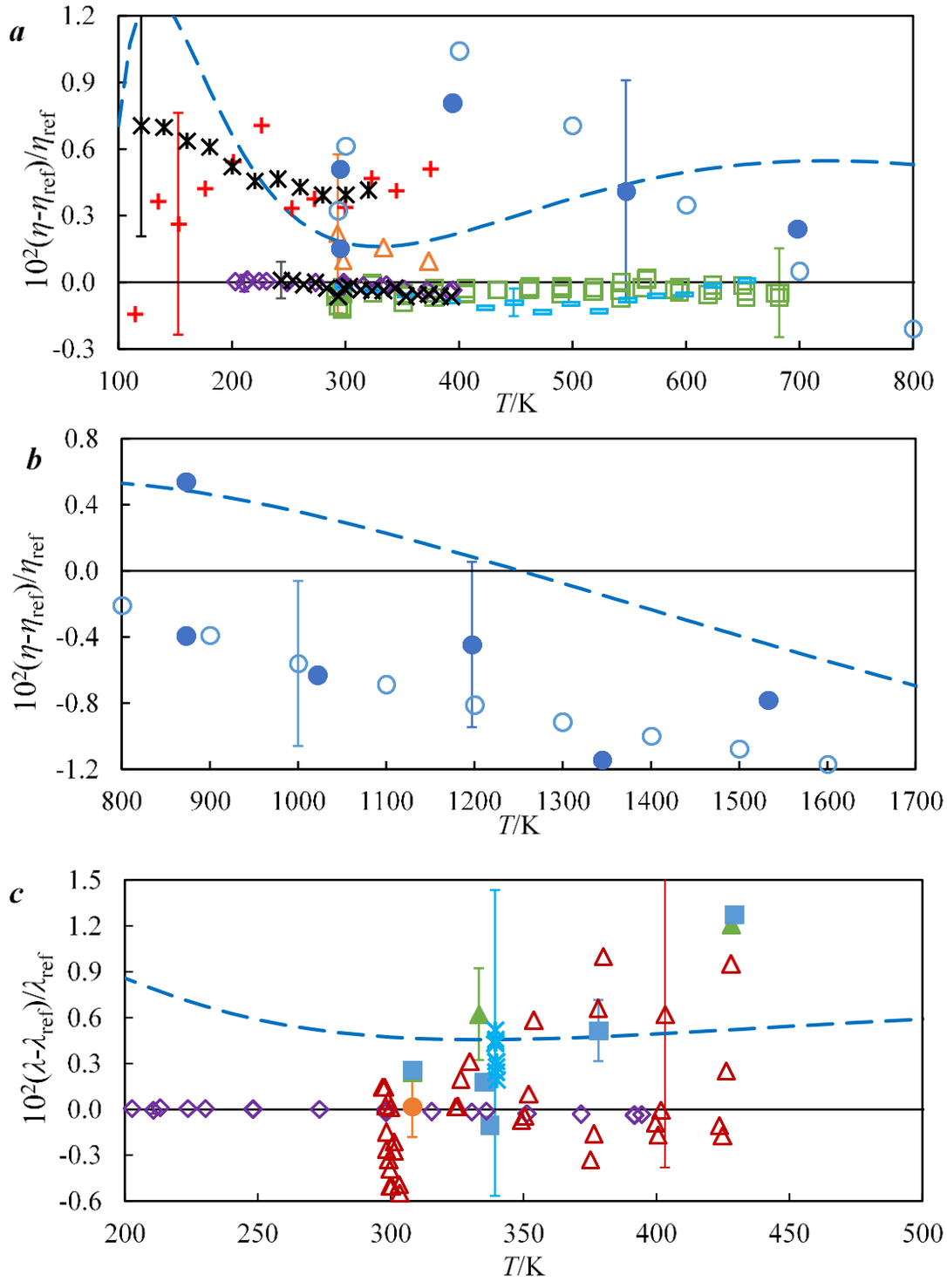

FIG. 8 ***a*** and ***b*** Viscosity deviations for argon. Experimental data: +, Clarke and Smith;[75] ○, Dawe and Smith;[70] ∗, Gough *et al.*;[63] △, Hurly *et al.*;[76] –, Lin *et al.*;[3] ◇, May *et al.*;[4] ●, Maitland and Smith;[77] □, Vogel;[12] ×, Zhang *et al.*[78] Blue long dash curve: model from Lemmon and Jacobsen[119] implemented in REFPROP 10. ***c*** Thermal conductivity deviations for argon. Experimental data: ●, Assael *et al.*;[31] ■, Haran *et al.*;[107] ◇, May *et al.*;[4] ▲, Millat *et al.*;[108] ∗, Roder *et al.*;[109] △, Sun *et al.*[110] Blue long dash curve: model from Lemmon and Jacobsen[119] implemented in REFPROP 10.

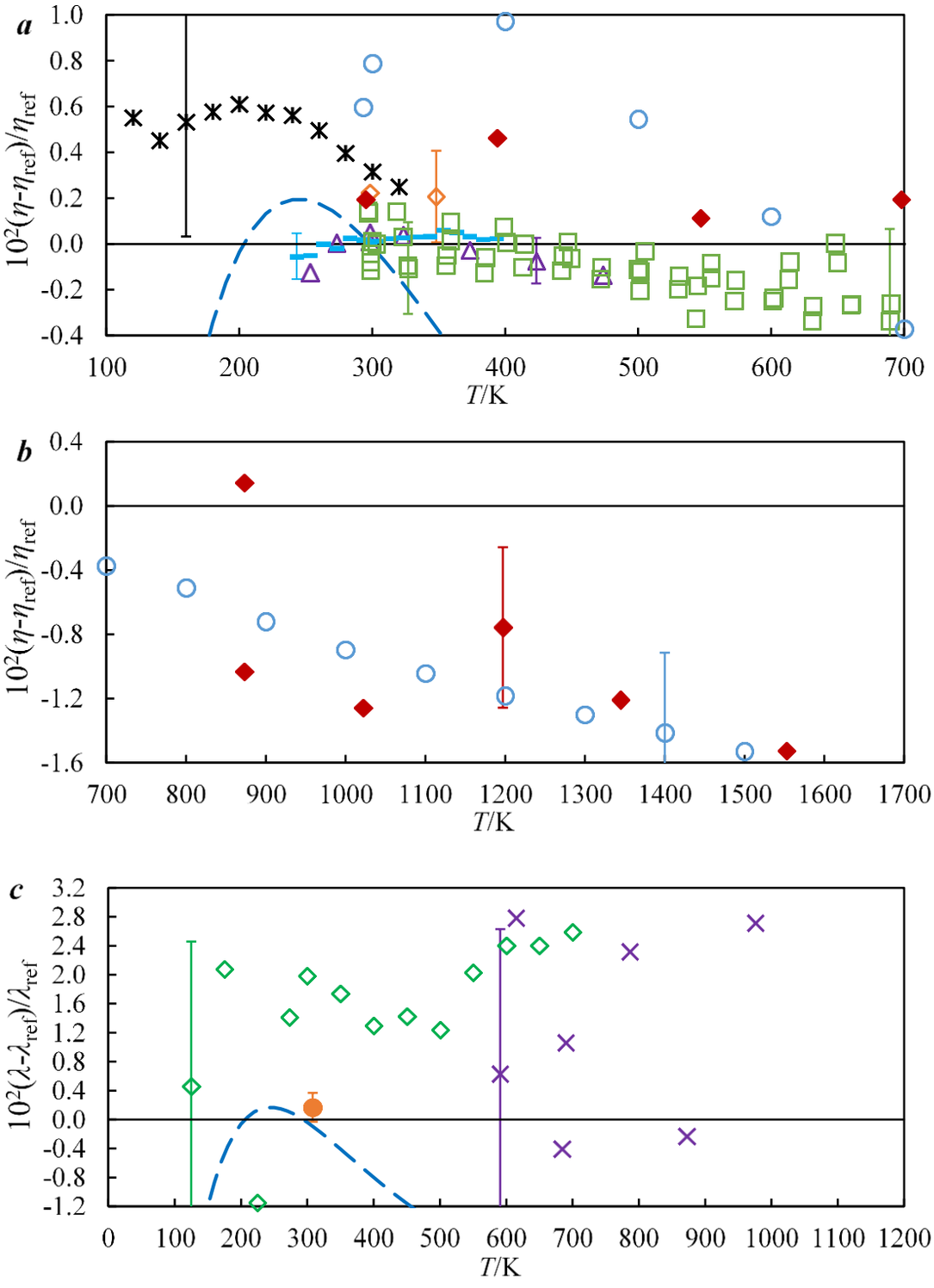

FIG. 9 ***a*** and ***b*** Viscosity deviations for krypton. Experimental data: ○, Dawe and Smith;[70] ∗, Gough *et al.*;[63] △, Humberg and Richter;[9] –, Lin *et al.*;[15] ◆, Maitland and Smith;[66] □, Vogel;[79] ◇, Wilhelm and Vogel.[80] Blue long dash curve: model from Huber[118] implemented in REFPROP 10. ***c*** Thermal conductivity deviations for krypton. Experimental data: ●, Assael *et al.*;[31] ◇, Vargaftik;[111] ×, Voshchinin *et al.*[112] Blue long dash curve: model from Huber[118] implemented in REFPROP 10.

For krypton, the viscosity data reported by Vogel[79] were re-evaluated based on the *ab initio* viscosities of argon. In Fig. 9*a*, the deviations of almost all the data from the reference correlations are within the experimental uncertainties, including the recent and highly accurate measurements of Vogel,[79] Lin *et al.*,[15] and Humberg and Richter.[9] For thermal conductivity, most of the measurements have a large uncertainty except the data from Assael *et al.*[31] at 308.15 K. In Fig. 9*b*, the thermal conductivity reference correlation represents the experimental data better than the *ab initio* calculations. Huber's model[118] is implemented in REFPROP 10 for krypton[115] but has relatively high uncertainties (3% for viscosity and 4% for thermal conductivity) and large deviations in Fig. 9. Within certain temperature ranges ((190 to 300) K for viscosity and (200 to 400) K for thermal conductivity), the predictions are within 1% of the reference correlations. Beyond these ranges, however, this model (which is designed to describe the data available at all pressures) is no longer in good agreement with the experimental data shown.

For xenon, the reference viscosity correlation represents almost all the data within their uncertainties, including the high-accuracy measurements by May *et al.*,[4] Vogel,[79] and Lin *et al.*[15] There are few high-quality data available for xenon's thermal conductivity. Results from May *et al.*[4] and Assael *et al.*[31] are consistent with the reference correlation over the temperature ranges covered by these data. The models of Huber[118] implemented in REFPROP 10 have moderate uncertainties for viscosity (1%) and thermal conductivity (3%), but are consistent within these limits with the reference correlations developed here.

For methane, the reference correlation represents most of the data within their uncertainties. *Ab initio* results for this system were originally obtained by Hellmann *et al.*[36] in 2008. However, their results deviate by 0.63% from the reference correlation and disagree with almost all the available data. In 2014, Hellmann *et al.*[38] re-scaled their results by a factor of 0.9955 based on the data reported Vogel.[13] This improves the agreement with the experimental measurements, although at some conditions these revised results still fall outside the uncertainty range of the high-quality data by Humberg *et al.*[10] and May *et al.*[4] The unpublished model from REFPROP 10 covers the temperature range of (100 to 910) K and is within 0.2% of the reference correlation between (200 to 400) K.

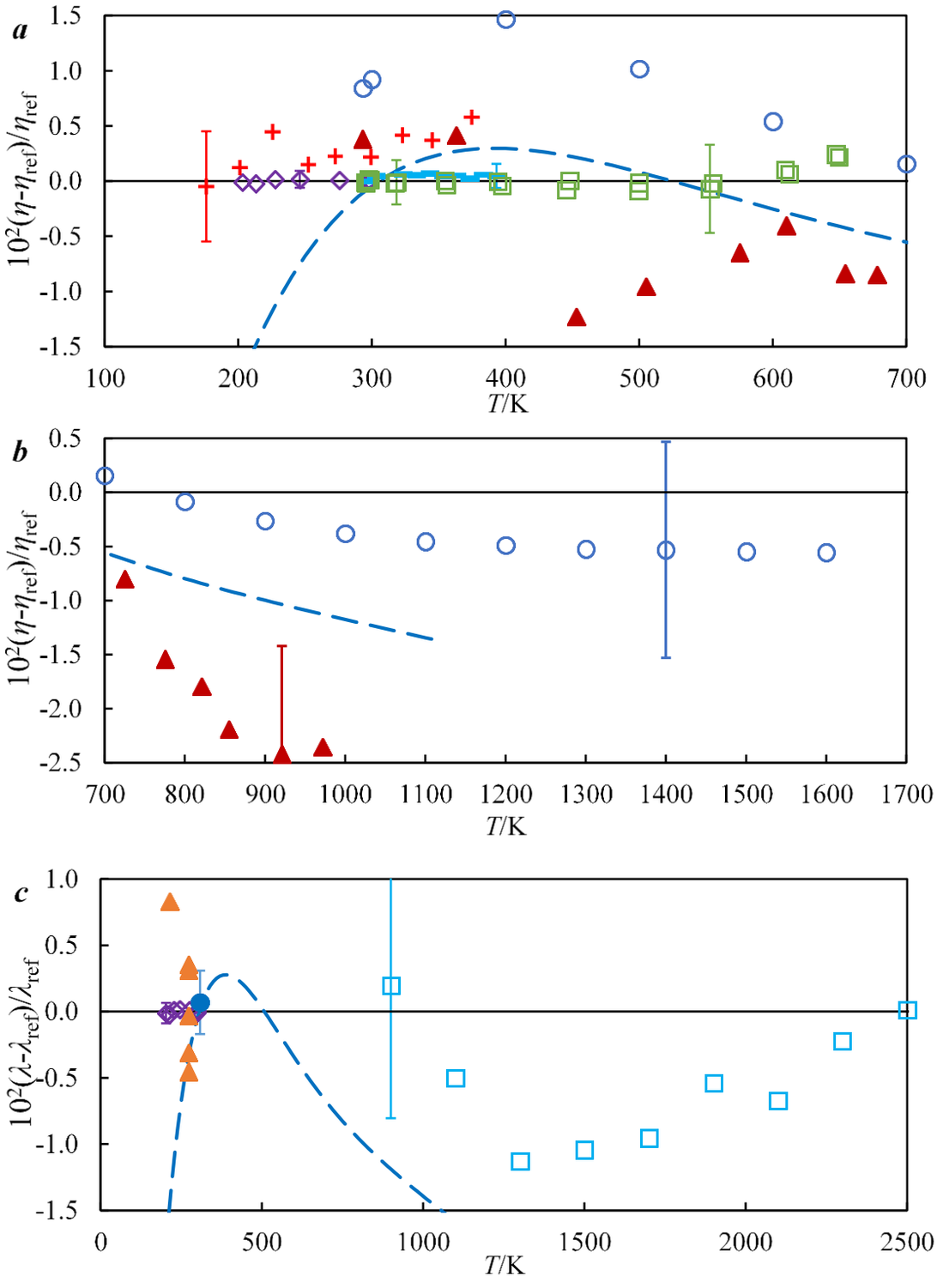

FIG. 10 ***a*** and ***b*** Viscosity deviations for xenon. Experimental data: +, Clarke and Smith;[75] ○, Dawe and Smith;[70] –, Lin *et al.*;[15] ◇, May *et al.*;[4] ▲, Rigby and Smith;[81] □, Vogel.[79] Blue long dash curve: model from Huber[118] implemented in REFPROP 10. ***c*** Thermal conductivity deviations for xenon. Experimental data: ●, Assael *et al.*;[31] ▲, Keyes (no reported or estimated uncertainty for this data);[113] ◇, May *et al.*;[4] □, Springer and Wingeier.[114] Blue long dash curve: model from Huber[118] implemented in REFPROP 10.

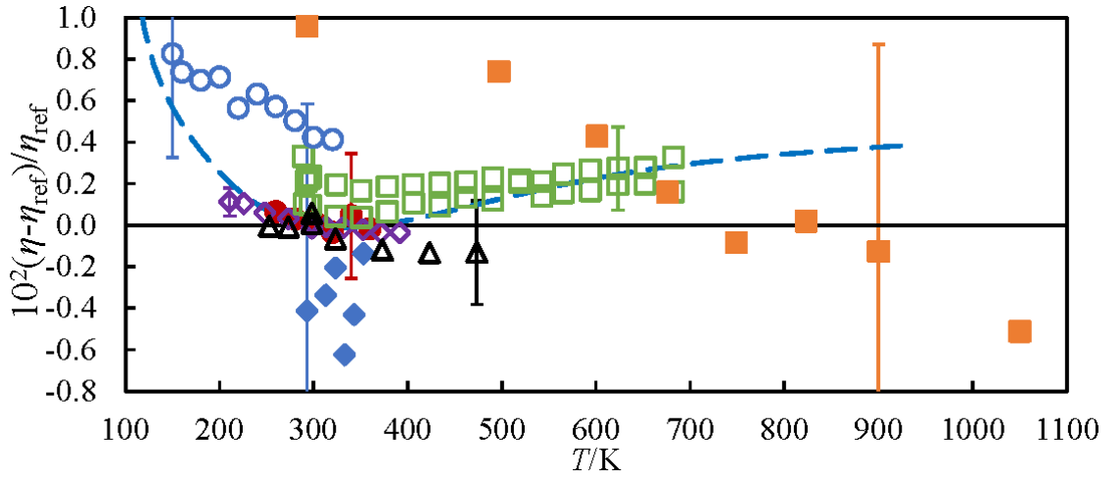

FIG. 11 Viscosity deviations for methane. Experimental data: ○, Gough *et al.*;[63] ■, Dawe *et al.*;[62] △, Humberg *et al.*;[10] ◇, May *et al.*;[4] ◆, Meerlender and Aziz;[82] ●, Schley *et al.*;[83] □, Vogel.[13] Blue long dash curve: unpublished model from REFPROP 10.

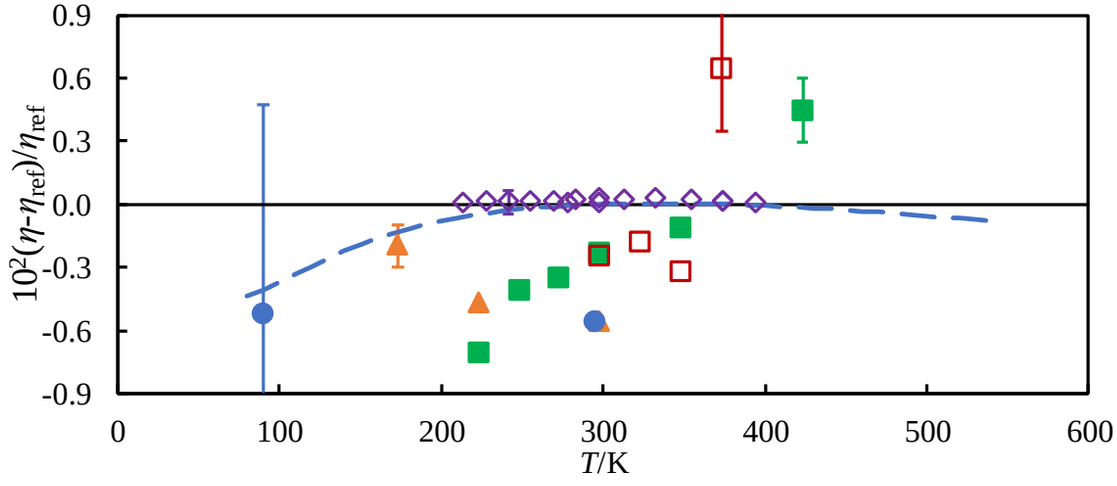

FIG. 12 Viscosity deviations for hydrogen. Experimental data: ■, Barua *et al.*;[84] ▲, Gracki;[85] □, Hongo and Iwasaki;[86] ◇, May *et al.*;[4] ●, Van Cleave and Maass.[87] Blue long dash curve: Model from Muzny *et al.*[120] implemented in REFPROP 10.

For hydrogen, the reference correlation is in excellent agreement with the data of May *et al.*[4] The data of Barua *et al.*[84] and Gracki[85] are mostly within 0.6%, which is larger than their claimed uncertainty. The model from Muzny *et al.*[120] implemented in REFPROP 10 has a low uncertainty because it was tuned to all the published hydrogen data available in 2012 including the *ab initio* potential results from Mehl *et al.*[29]

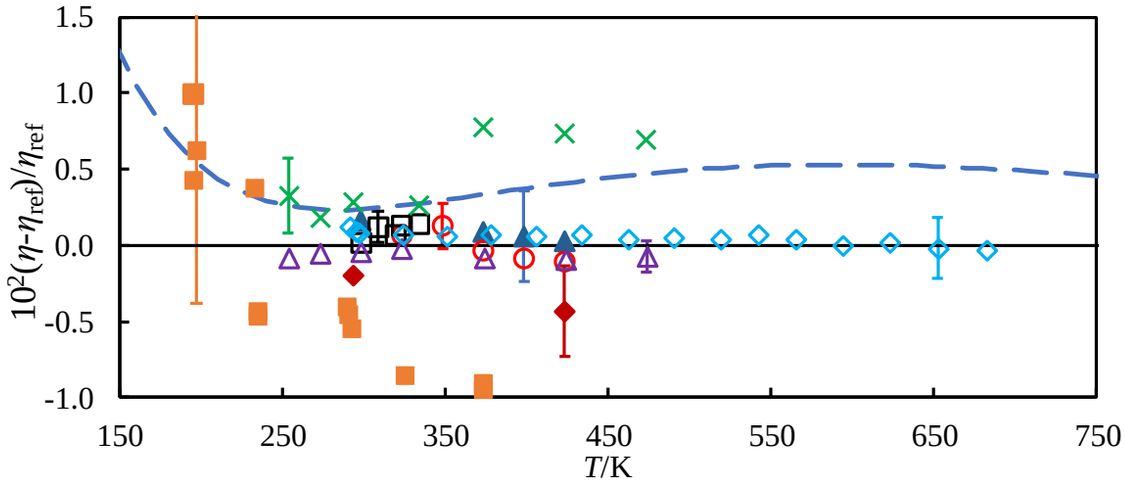

FIG. 13 Viscosity deviations for nitrogen. Experimental data: ×, El Hawary;[88] □, Hoogland *et al.*;[89] △, Humberg *et al.*;[8] ○, Kestin *et al.*;[56] ▲, Seibt *et al.*;[90] ◇, Seibt *et al.*;[67] ■, Trautz and Baumann;[91] ◇, Vogel.[14] Blue long dash curve: model from Lemmon and Jacobsen[119] implemented in REFPROP 10.

For nitrogen, about 80% of data are within 1% of the reference correlation, with excellent agreement exhibited by the high-quality data of Humberg *et al.*[8] and Vogel.[14] The model from Lemmon and Jacobsen[119] implemented in REFPROP 10 has a relative uncertainty of 0.5% for the dilute gas and generally agrees with the reference correlation within this bound.

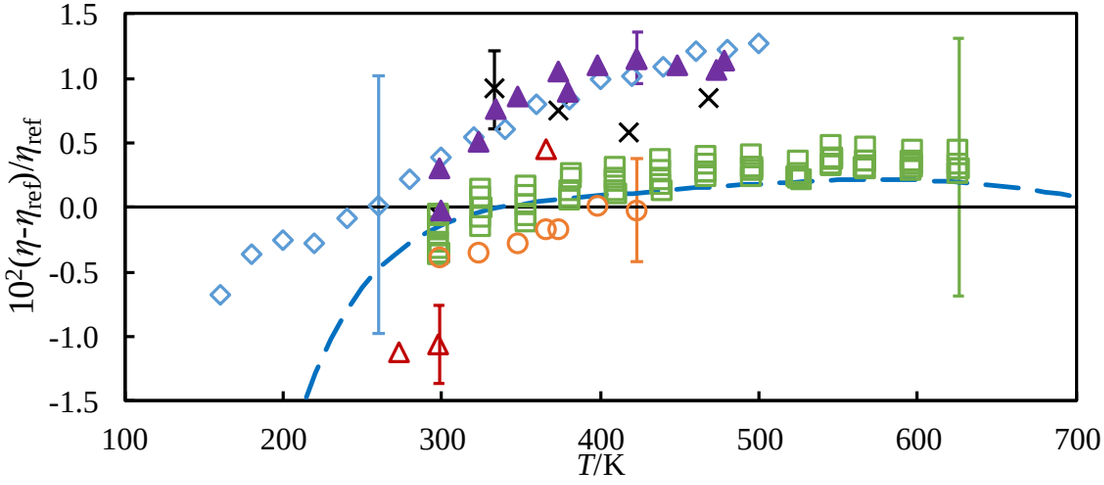

FIG. 14 Viscosity deviations for propane. Experimental data: ×, Abe *et al.*;[95] ◇, Holland *et al.*;[96] ▲, Kestin *et al.*;[58] △, Seibt *et al.*;[97] □, Vogel;[57] ○, Wilhelm and Vogel.[98] Blue long dash curve: model from Vogel and Herrmann[121] implemented in REFPROP 10.

The relatively complex structure of the propane molecule means that *ab initio* results are of larger uncertainty compared to those for simpler gases. The reference viscosity correlation has an uncertainty 20% smaller than the *ab initio* values, and is consistent with the majority of the data from Vogel,[57] Wilhelm and Vogel,[98] and Holland *et al.*[96] within the experimental uncertainties. Vogel and Herrmann's model[121] implemented in REFPROP 10 was tuned to Vogel's reported data[57] for the dilute gas at 273 K < T < 625 K, and has a stated relative uncertainty of 1%.

Results for ethane are only given in the table as a deviation plot from the *ab initio* results as given by Hellmann.[37] As mentioned in Sec. 3, the reference correlation is based entirely on the *ab initio* calculated values for ethane.

6. Conclusions

This work makes two primary contributions to the determination of dilute gas transport properties over wide ranges of temperature. Updated values of the dilute gas viscosities for H_2, Ar, CH_4, and Xe measured in 2007 by May *et al.*[4] were calculated using the highly accurate reference viscosity for helium calculated *ab initio* in 2012 by Cencek *et al.*;[32] this reduced the uncertainties of the measured data by between (23 and 55) %. Additionally, new reference correlations for the dilute gas viscosity of ten gases spanning the temperature range at least (150 to 1200) K were developed by combining *ab initio* calculations for each gas with the experimental reference viscosity ratios at 298 K. For fluids other than helium, this approach reduces the uncertainty currently achievable via a direct *ab initio* calculation by up to 85%: between (200 to 400) K, the relative uncertainties of the reference viscosity correlations range from about 0.05% for Kr and H_2 to about 0.3% for N_2 and propane. New reference correlations for the dilute gas thermal conductivity of five noble gases were also developed, covering the temperature range at least (100 to 5000) K with relative uncertainties ranging from 0.04% for argon to 0.2% for xenon. These reference correlations generally represent the measured data (corrected to dilute gas conditions) available for these fluids within the experimental uncertainty. The hybrid approach detailed in this work should be readily applicable to additional fluids once their transport properties are described by suitable *ab initio* calculations.

Supplementary Material

A Supplementary Information document is provided which presents alternative reference correlations with slightly lower precision that extrapolate to low and high temperatures as expected by theory. The Supplementary Information also presents further detail about the uncertainty of the reference ratio correlations as a function of temperature.

Acknowledgements

The authors thank Robert Hellmann from the University of Rostock for providing the updated argon *ab initio* transport property values. We are grateful to Dr. Hongzhou Tian from Nanjing University for assistance with the data regression software 1stOpt access. One of us (X.X.) was supported by a UWA Ad Hoc Postgraduate Scholarship and Faculty Scholarship for International Research Fees.

7. References

1. J. C. Rainwater and D. G. Friend, Phys. Rev. A **36**, 4062 (1987).

2. M. J. Assael, A. E. Kalyva, S. A. Monogenidou, M. L. Huber, R. A. Perkins, D. G. Friend, and E. F. May, J. Phys. Chem. Ref. Data **47**, 021501 (2018).

3. H. Lin, X. J. Feng, J. T. Zhang, and L. Can, J. Chem. Phys. **141**, 234311 (2014).

4. E. F. May, R. F. Berg, and M. R. Moldover, Int. J. Thermophys. **28**, 1085 (2007).

5. M. R. Moldover, IEEE Trans. Instrum. Meas. **38**, 217 (1989).

6. J. J. Segovia, D. Lozano-Martín, M. C. Martín, C. R. Chamorro, M. A. Villamañán, E. Pérez, C. G. Izquierdo, and D. del Campo, Metrologia **54**, 663 (2017).

7. A. Grant, in *Phys. Today* (AIP Publishing, 2018, DOI 10.1063/PT.6.2.20181116a), Vol. Politics & Policy

8. K. Humberg, M. Richter, J. P. M. Trusler, and R. Span, J. Chem. Thermodyn. **120**, 191 (2018).

9. K. Humberg and M. Richter, Ind. Eng. Chem. Res. **58**, 8878 (2019).

10. K. Humberg, M. Richter, J. P. M. Trusler, and R. Span, (Ruhr-Universität Bochum, in preparation, 2019).

11. G. F. Newell, Z. Angew. Math. Phys. **10**, 160 (1959).

12. E. Vogel, Int. J. Thermophys. **31**, 447 (2010).

13. E. Vogel, J. Chem. Eng. Data **56**, 3265 (2011).

14. E. Vogel, Int. J. Thermophys. **33**, 741 (2012).

15. H. Lin, J. Che, J. T. Zhang, and X. J. Feng, Fluid Phase Equilib. **418**, 198 (2016).

16. E. Vogel, B. Jäger, R. Hellmann, and E. Bich, Mol. Phys. **108**, 3335 (2010).

17. E. F. May, M. R. Moldover, R. F. Berg, and J. J. Hurly, Metrologia **43**, 247 (2006).

18. A. Laesecke and C. D. Muzny, Int. J. Thermophys. **38**, 182 (2017).

19. A. Laesecke and C. D. Muzny, Int. J. Thermophys. (Erratum 1) **39**, 34 (2018).

20. A. Laesecke and C. D. Muzny, Int. J. Thermophys. (Erratum 2) **39**, 52 (2018).

21. S. Chapman and T. G. Cowling, *The mathematical theory of non-uniform gases: an account of the kinetic theory of viscosity, thermal conduction and diffusion in gases*. (Cambridge University Press, 1970).

22. E. Bich, R. Hellmann, and E. Vogel, Mol. Phys. **106**, 813 (2008).

23. E. Bich, R. Hellmann, and E. Vogel, Mol. Phys. (Erratum) **106**, 1107 (2008).

24. R. Hellmann, E. Bich, E. Vogel, A. S. Dickinson, and V. Vesovic, J. Chem. Phys. **130**, 124309 (2009).

25. R. Hellmann, Mol. Phys. **111**, 387 (2013).

26. B. Jäger, R. Hellmann, E. Bich, and E. Vogel, J. Chem. Phys. **144**, 114304 (2016).

27. R. Hellmann, J. Chem. Phys. **146**, 114304 (2017).

28. R. Hellmann, B. Jäger, and E. Bich, J. Chem. Phys. **147**, 034304 (2017).

29. J. B. Mehl, M. L. Huber, and A. H. Harvey, Int. J. Thermophys. **31**, 740 (2010).

30. R. F. Berg and M. R. Moldover, J. Phys. Chem. Ref. Data **41**, 043104 (2012).

31. M. J. Assael, M. Dix, A. Lucas, and W. A. Wakeham, J. Chem. Soc., Faraday Trans. 1 **77**, 439 (1981).

32. W. Cencek, M. Przybytek, J. Komasa, J. B. Mehl, B. Jeziorski, and K. Szalewicz, J. Chem. Phys. **136**, 224303 (2012).

33. J. J. Hurly and J. B. Mehl, J. Res. Natl. Inst. Stand. Technol. **112**, 75 (2007).

34. S. J. Boyes, Chem. Phys. Lett. **221**, 467 (1994).

35. A. K. Dham, W. J. Meath, A. R. Allnatt, R. A. Aziz, and M. J. Slaman, Chem. Phys. **142**, 173 (1990).

36. R. Hellmann, E. Bich, E. Vogel, A. S. Dickinson, and V. Vesovic, J. Chem. Phys. **129**, 064302 (2008).

37. R. Hellmann, J. Chem. Eng. Data **63**, 470-481 (2018).

38. R. Hellmann, E. Bich, E. Vogel, and V. Vesovic, J. Chem. Phys. **141**, 224301 (2014).

39. R. Hellmann, (Private Communication, 2019).

40. J. J. Hurly and M. R. Moldover, J. Res. Natl. Inst. Stand. Technol. **105**, 667 (2000).

41. E. Bich, R. Hellmann, and E. Vogel, Mol. Phys., 3035 (2007).

42. M. J. Slaman and R. A. Aziz, Chem. Eng. Commun. **104**, 139 (1991).

43. K. Patkowski, G. Murdachaew, C.-M. Fou, and K. Szalewicz, Mol. Phys. **103**, 2031 (2005).

44. R. A. Aziz, J. Chem. Phys. **99**, 4518 (1993).

45. R. A. Aziz and M. J. Slaman, Chem. Eng. Commun. **78**, 153 (1989).

46. J. M. Waldrop, B. Song, K. Patkowski, and X. Wang, J. Chem. Phys. **142**, 204307 (2015).

47. S. M. Cybulski and R. R. Toczyłowski, J. Chem. Phys. **111**, 10520 (1999).

48. L. Zarkova, U. Hohm, and M. Damyanova, J. Phys. Chem. Ref. Data **35**, 1331 (2006).

49. E. Nemati-Kande and A. Maghari, J. Iran. Chem. Soc. **13**, 1225 (2016).

50. M. H. K. Jafari, A. Maghari, and S. Shahbazian, Chem. Phys. **314**, 249 (2005).

51. P. Diep and J. K. Johnson, J. Chem. Phys. **112**, 4465 (2000).

52. P. Diep and J. K. Johnson, J. Chem. Phys. (Erratum) **113**, 3480 (2000).

53. P. Wind and I. Røeggen, Chem. Phys. **174**, 345 (1993).

54. I. F. Silvera and V. V. Goldman, J. Chem. Phys. **69**, 4209 (1978).

55. J. B. Mehl, *Quantum-Mechanical Calculations of Hydrogen Transport Properties from Pair Potentials* (unpublished report, 2007).

56. J. Kestin, S. T. Ro, and W. A. Wakeham, Ber. Bunsenges. Phys. Chem. **86**, 753 (1982).

57. E. Vogel, Int. J. Thermophys. **16**, 1335 (1995).

58. J. Kestin, H. E. Khalifa, and W. A. Wakeham, J. Chem. Phys. **66**, 1132 (1977).

59. E. Vogel, R. Span, and S. Herrmann, J. Phys. Chem. Ref. Data **44**, 043101 (2015).

60. R. F. Berg, Metrologia **43**, 183 (2006).

61. A. G. Clarke and E. B. Smith, J. Chem. Phys. **51**, 4156 (1969).

62. R. A. Dawe, G. C. Maitland, M. Rigby, and E. B. Smith, Trans. Faraday Soc. **66**, 1955 (1970).

63. D. W. Gough, G. P. Matthews, and E. B. Smith, J. Chem. Soc., Faraday Trans. 1 **72**, 645 (1976).

64. J. Kestin, H. E. Khalifa, S. T. Ro, and W. A. Wakeham, Physica A **88**, 242 (1977).

65. J. Kestin, H. E. Khalifa, and W. A. Wakeham, Physica A **90**, 215 (1978).

66. G. C. Maitland and E. B. Smith, J. Chem. Soc., Faraday Trans. 1 **70**, 1191 (1974).

67. D. Seibt, S. Herrmann, E. Vogel, E. Bich, and E. Hassel, J. Chem. Eng. Data **54**, 2626 (2009).

68. Y. Tanaka, M. Nakajima, H. Kubota, and T. Makita, J. Chem. Eng. Jpn **13**, 155 (1980).
69. E. Vogel, E. Bastubbe, and S. Rohde, Wiss. Z. W.-Pieck-Univ. Rostock **33**, 34 (1984).
70. R. A. Dawe and E. B. Smith, J. Chem. Phys. **52**, 693 (1970).
71. R. S. Edwards, Proc. R. Soc. Lond. A Math. Phys. Sci. **119**, 578 (1928).
72. C. Evers, H. W. Lösch, and W. Wagner, Int. J. Thermophys. **23**, 1411 (2002).
73. H. L. Johnston and E. R. Grilly, J. Phys. Chem. **46**, 948 (1942).
74. M. Trautz and H. Zimmermann, Ann Phys **414**, 189 (1935).
75. A. G. Clarke and E. B. Smith, J. Chem. Phys. **48**, 3988 (1968).
76. J. J. Hurly, K. A. Gillis, J. B. Mehl, and M. R. Moldover, Int. J. Thermophys. **24**, 1441 (2003).
77. G. C. Maitland and E. B. Smith, J. Chem. Eng. Data **17**, 150 (1972).
78. J. T. Zhang, H. Lin, and J. Che, Metrologia **50**, 377 (2013).
79. E. Vogel, Int. J. Thermophys. **37**, 63 (2016).
80. J. Wilhelm and E. Vogel, Int. J. Thermophys. **21**, 301 (2000).
81. M. Rigby and E. B. Smith, Trans. Faraday Soc. **62**, 54 (1966).
82. G. Meerlender and N. A. Aziz, Rheol. Acta **11**, 19 (1972).
83. P. Schley, M. Jaeschke, C. Küchenmeister, and E. Vogel, Int. J. Thermophys. **25**, 1623 (2004).
84. A. K. Barua, M. Afzal, G. P. Flynn, and J. Ross, J. Chem. Phys. **41**, 374 (1964).
85. J. A. Gracki, G. P. Flynn, and J. Ross, J. Chem. Phys. **51**, 3856 (1969).
86. M. Hongo and H. Iwasaki, Rev. Phys. Chem. Jpn. **48**, 1 (1978).
87. A. B. V. Cleave and O.Maass, Can. J. Res. **13**, 384 (1935).
88. T. El Hawary, *Messung der Dichte und Viskosität in der Gasphase vonMethan, Stickstoff und Methan-Stickstoff-Gemischen mit einer weiterentwickelten kombinierten Viskositäts-Dichte-Messanlage und einer neuen Viskositätsmessanlage für geringe Gasdichten*, PhD thesis, Ruhr-Universität Bochum, 2009.
89. J. H. B. Hoogland, H. R. Van Den Berg, and N. J. Trappeniers, Physica A **134**, 169 (1985).
90. D. Seibt, E. Vogel, E. Bich, D. Buttig, and E. Hassel, J. Chem. Eng. Data **51**, 526 (2006).
91. M. Trautz and P. B. Baumann, Ann. Phys. **394**, 733 (1929).
92. H. Iwasaki and M. Takahashi, J. Chem. Phys. **74**, 1930 (1981).
93. J. Wilhelm, D. Seibt, E. Vogel, D. Buttig, and E. Hassel, J. Chem. Eng. Data **56**, 1730 (2011).
94. S. Herrmann, R. Hellmann, and E. Vogel, J. Phys. Chem. Ref. Data **47**, 023103 (2018).
95. Y. Abe, J. Kestin, H. E. Khalifa, and W. A. Wakeham, Physica A **93**, 155 (1978).
96. P. M. Holland, H. J. M. Hanley, K. E. Gubbins, and J. M. Haile, J. Phys. Chem. Ref. Data **8**, 559 (1979).
97. D. Seibt, K. Voß, S. Herrmann, E. Vogel, and E. Hassel, J. Chem. Eng. Data **56**, 1476 (2011).
98. J. Wilhelm and E. Vogel, J. Chem. Eng. Data **46**, 1467 (2001).
99. E. B. Charles and S. B. Richard, J. Chem. Phys. **40**, 1523 (1964).
100. J. Kestin, R. Paul, A. A. Clifford, and W. A. Wakeham, Physica A **100**, 349 (1980).
101. P. Mukhopadhyay and A. K. Barua, Br. J. Appl. Phys. **18**, 635 (1967).

102. M. Mustafa, M. Ross, R. D. Trengove, W. A. Wakeham, and M. Zalaf, Physica A **141**, 233 (1987).

103. J. J. De Groot, J. Kestin, H. Sookiazian, and W. A. Wakeham, Physica A **92**, 117 (1978).

104. F. G. Keyes, Trans. ASME **76**, 809 (1954).

105. J. V. Sengers, W. T. Bolk, and C. J. Stigter, Physica **30**, 1018 (1964).

106. R. M. Sevast'yanov and N. A. Zykov, J. Eng. Phys. **34**, 79 (1978).

107. K. N. Haran, G. C. Maitland, M. Mustafa, and W. A. Wakeham, Ber. Bunsenges. Phys. Chem. **87**, 657 (1983).

108. J. Millat, M. Mustafa, M. Ross, W. A. Wakeham, and M. Zalaf, Physica A **145**, 461 (1987).

109. H. M. Roder, R. A. Perkins, A. Laesecke, and C. A. Nieto de Castro, J. Res. Natl. Inst. Stand. Technol. **105**, 221 (2000).

110. L. Sun, J. E. S. Venart, and R. C. Prasad, Int. J. Thermophys. **23**, 357 (2002).

111. N. B. Vargaftik, *Dictionary of Thermophysical Properties of Gases and Liquids*. (Moscow, 1972).

112. A. A. Voshchinin, V. V. Kerzhentsev, E. L. Studnikov, and L. V. Yakush, Inzh. Fiz. Zh. **28**, 821 (1975).

113. F. G. Keyes, Trans. Am. Soc. Mech. Eng. **77**, 1395 (1955).

114. G. Ś. Springer and E. W. Wingeier, J. Chem. Phys. **59**, 2747 (1973).

115. E. W. Lemmon, I. H. Bell, M. L. Huber, and M. O. McLinden, *NIST Standard Reference Database 23: Reference Fluid Thermodynamic and Transport Properties-REFPROP, Version 10* (National Institute of Standards and Technology, Gaithersburg, MD, 2018).

116. V. D. Arp, R. D. McCarty, and D. G. Friend, NIST Tech. Note 1334, *Thermophysical properties of helium-4 from 0.8 to 1500 K with pressures to 2000 MPa*. (U.S. Government Printing Office, Washington, DC, 1998).

117. B. A. Hands and V. D. Arp, Cryogenics **21**, 697 (1981).

118. M. L. Huber, NISTIR 8209, *Models for Viscosity, Thermal Conductivity, and Surface Tension of Selected Pure Fluids as Implemented in REFPROP v10.0*. (National Institute of Standards and Technology, 2018).

119. E. W. Lemmon and R. T. Jacobsen, Int. J. Thermophys. **25**, 21 (2004).

120. C. D. Muzny, M. L. Huber, and A. F. Kazakov, J. Chem. Eng. Data **58**, 969 (2013).

121. E. Vogel and S. Herrmann, J. Phys. Chem. Ref. Data **45**, 043103 (2016).

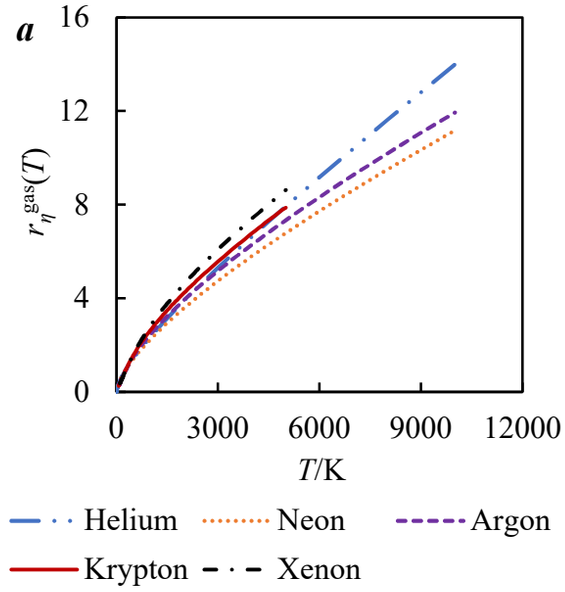

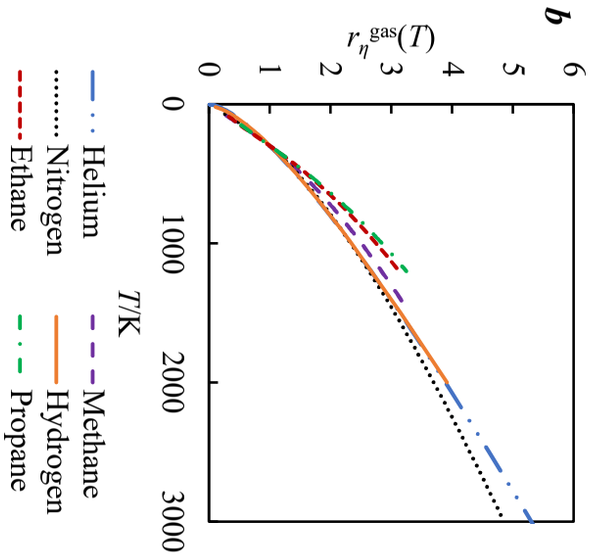

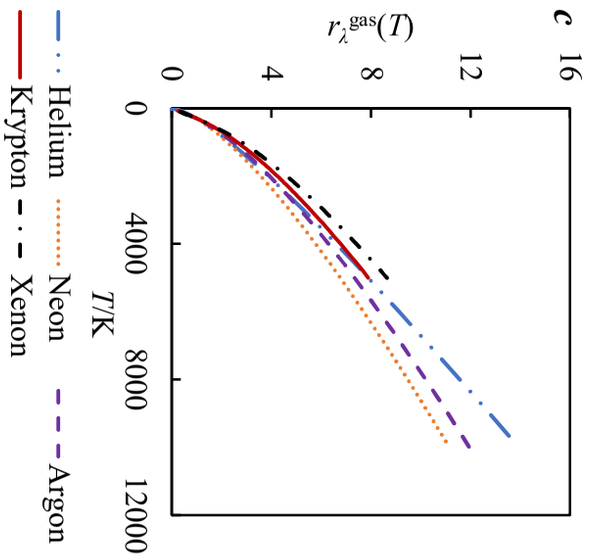

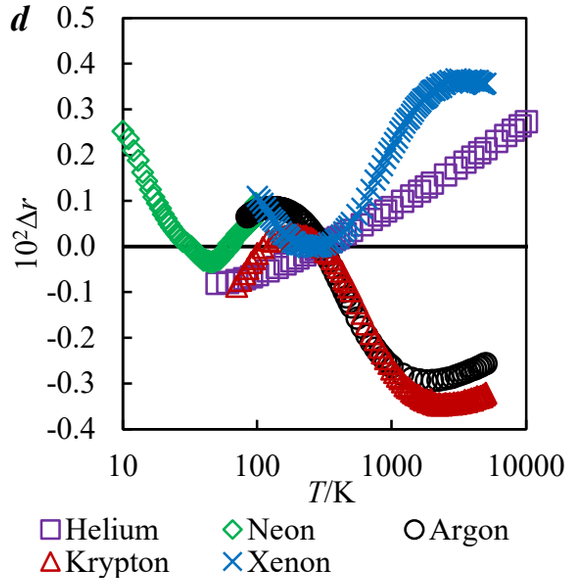

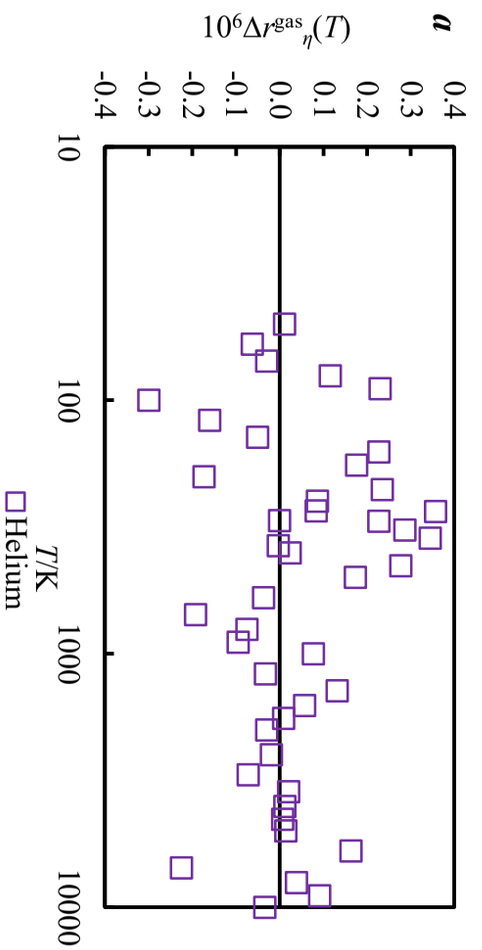

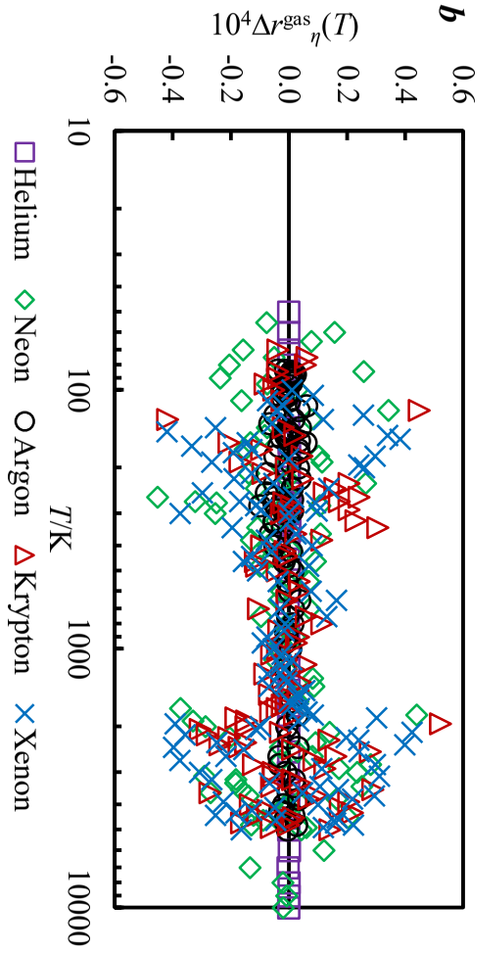

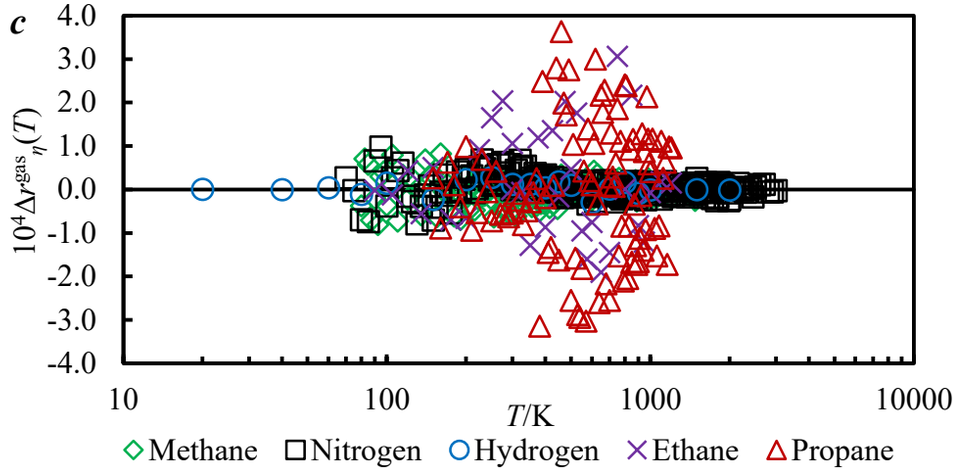

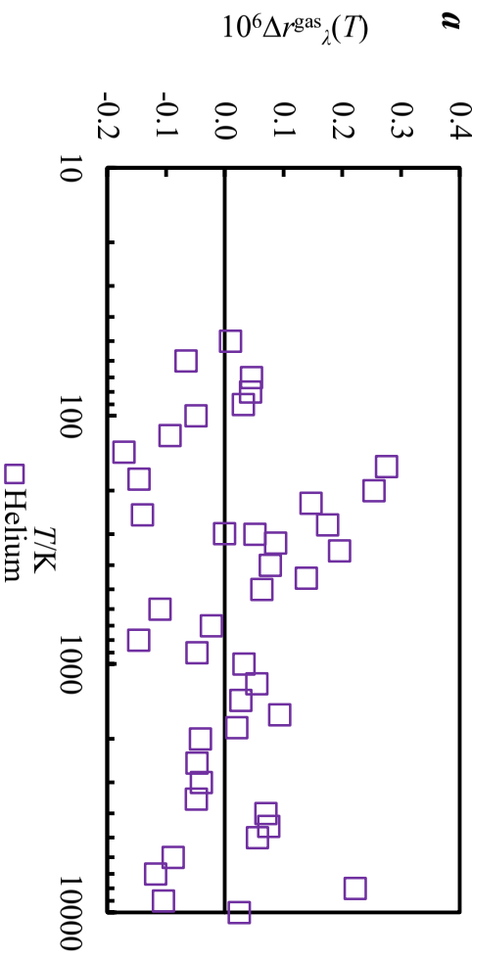

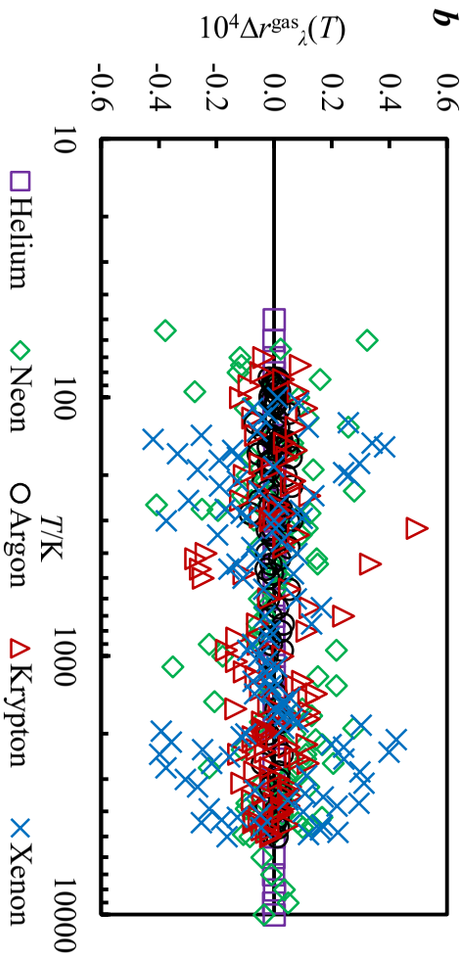

Journal of Physical and Chemical Reference Data

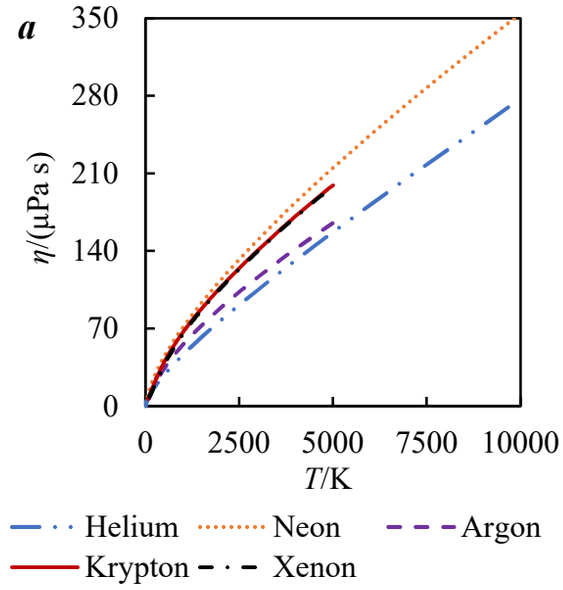

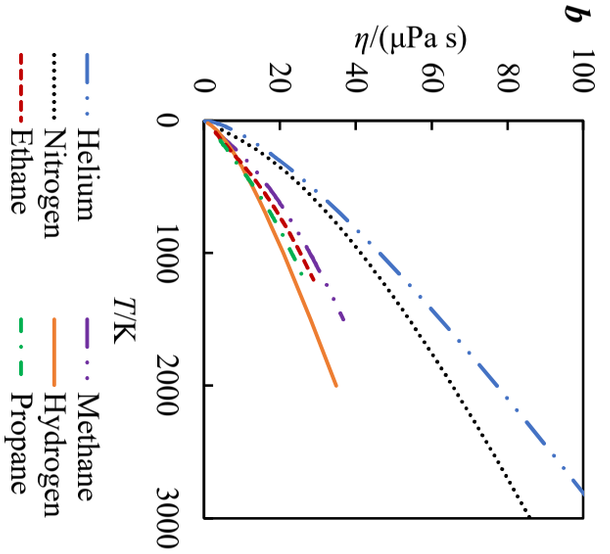

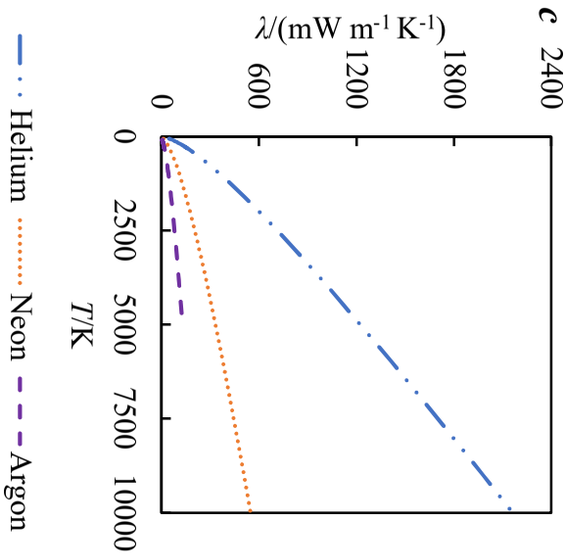

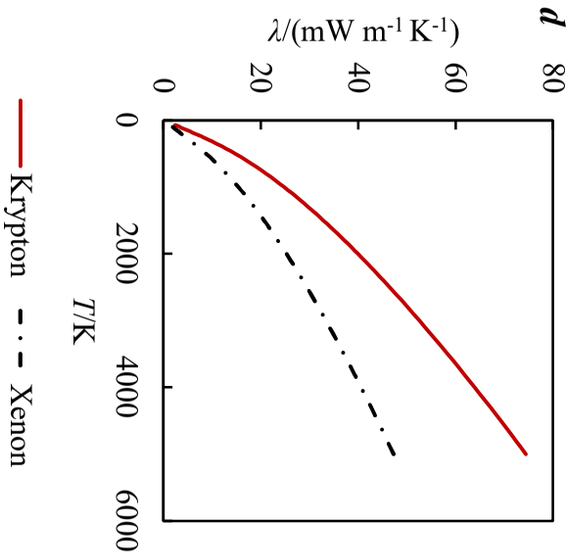

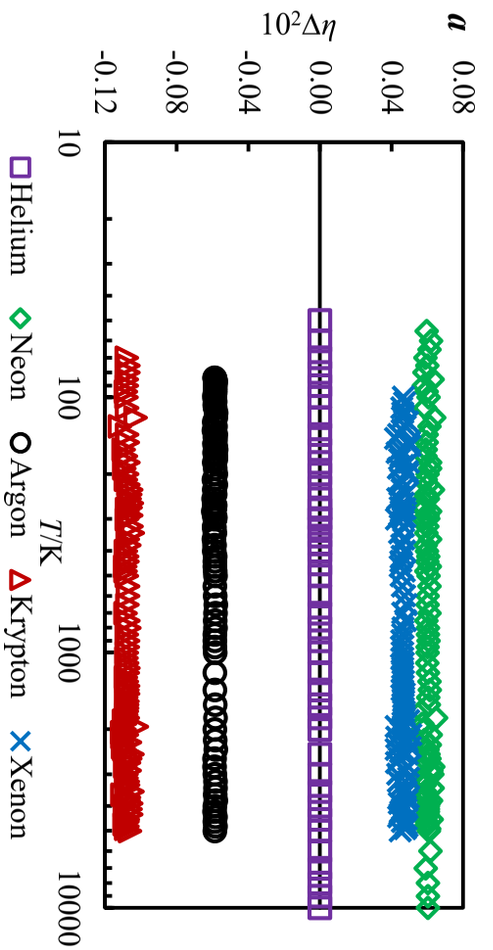

Journal of Physical and Chemical Reference Data